HHS Public Access

Author manuscript

J Immunol. Author manuscript; available in PMC 2020 September 15.

Published in final edited form as:

J Immunol. 2020 March 15; 204(6): 1674–1688. doi:10.4049/jimmunol.1901194.

GCNT1-mediated O-glycosylation of the sialomucin CD43 is a sensitive indicator of Notch signaling in activated T cells

Eric Perkey[*,†], **Dave Maurice De Sousa**[‡], **Léolène Carrington**[§], **Jooho Chung**[†], **Alexander Dils**[†], **David Granadier**[†], **Ute Koch**[‖], **Freddy Radtke**[‖], **Burkhard Ludewig**[#], **Bruce R. Blazar**[**], **Christian W. Siebel**[††], **Todd V. Brennan**[‡‡], **Jeffrey Nolz**[§§], **Nathalie Labrecque**[‡], **Ivan Maillard**[§]

[*]Graduate Program in Cellular and Molecular Biology, University of Michigan, Ann Arbor, MI

[†]Life Sciences Institute, University of Michigan, Ann Arbor, MI

[‡]Maisonneuve-Rosemont Research Center, Département de Médecine et Département de Microbiologie, Infectiologie et Immunologie, Université de Montréal, Montréal, Québec, Canada

[§]Division of Hematology-Oncology, Department of Internal Medicine, University of Pennsylvania Perelman School of Medicine, Philadelphia, PA

[‖]EPFL, Lausanne, Switzerland, University of Minnesota, Minneapolis, MN

[#]Institute of Immunobiology, Kantonsspital St. Gallen, Switzerland, University of Minnesota, Minneapolis, MN

[**]Department of Pediatrics, Division of Blood and Marrow Transplantation, University of Minnesota, Minneapolis, MN

[††]Genentech, South San Francisco, CA

[‡‡]Cedars-Sinai Medical Center, Los Angeles, CA

[§§]Oregon Health and Sciences University, Portland, OR.

Abstract

Notch signaling is emerging as a critical regulator of T cell activation and function. However, there is no reliable cell surface indicator of Notch signaling across activated T cell subsets. Here we show that Notch signals induce upregulated expression of the *Gcnt1* glycosyl-transferase gene in T cells mediating graft-versus-host disease (GVHD) after allogeneic bone marrow transplantation (allo-BMT) in mice. To determine if *Gcnt1*-mediated O-glycosylation could be used as a Notch signaling reporter, we quantified the core-2 O-glycoform of CD43 in multiple T cell subsets during GVHD. Pharmacological blockade of Delta-like Notch ligands abrogated core-2 O-glycosylation in a dose-dependent manner after allo-BMT, both in donor-derived $CD4^+$ and $CD8^+$ effector T cells, and in $Foxp3^+$ regulatory T cells. CD43 core-2 O-glycosylation depended on cell-intrinsic canonical Notch signals and identified $CD4^+$ and $CD8^+$ T cells with high cytokine-

Co-corresponding authors: Nathalie Labrecque, Maisonneuve-Rosemont Hospital Research Center, 5415 Boulevard de l'Assomption, Montréal, QC H1T 2M4, Canada. nathalie.labrecque@umontreal.ca and Ivan Maillard, MD-PhD, 421 Curie Blvd, BRB-2/3 Rm 451, University of Pennsylvania, Philadelphia, PA 19104. Tel 215-746-2929. Fax: 215-746-5511. imaillar@pennmedicine.upenn.edu.

producing ability. *Gcnt1*-deficient T cells still drove lethal alloreactivity, showing that core-2 O-glycosylation predicted, but did not cause Notch-dependent T cell pathogenicity. Using core-2 O-glycosylation as a marker of Notch signaling, we identified Ccl19-Cre$^+$ fibroblastic stromal cells as critical sources of Delta-like ligands in graft-versus-host responses irrespective of conditioning intensity. Core-2 O-glycosylation also reported Notch signaling in CD8$^+$ T cell responses to dendritic cell immunization, *Listeria* infection, and viral infection. Thus, we uncovered a role for Notch in controlling core-2 O-glycosylation and identified a cell surface marker to quantify Notch signals in multiple immunological contexts. Our findings will help refine our understanding of the regulation, cellular source, and timing of Notch signals in T cell immunity.

Introduction

Notch signaling is an evolutionarily conserved juxtracrine signaling pathway. Interaction of Notch receptors (Notch1-4) with agonistic ligands of the Delta-like or Jagged families leads to proteolytic release of the Notch intracellular domain, followed by its translocation to the nucleus where it mediates the transcriptional activation of Notch target genes. T cell development requires Delta-like4/Notch1 interactions in the thymus. In addition, Notch has emerged as a critical regulator of mature CD4$^+$ and CD8$^+$ T cell activation, differentiation, and effector function in the periphery (1). T cells incapable of receiving Notch signals showed reduced acute protective functions in mouse models of intracellular bacterial (2), viral (3), fungal (4), and parasitic infection (5), as well as in selected tumor models (6, 7). Notch also drives pathogenic T cell functions in mouse models of T cell-mediated acute GVHD (8–11), chronic GVHD (12), organ rejection (13–15), and multiple sclerosis (16, 17). Despite the multiple immunological effects of Notch signaling in T cells, it has remained impossible to prospectively identify individual cells experiencing active Notch signaling, a major limitation to studying the detailed impact and regulation of the Notch pathway in vivo.

In mouse models of allogeneic bone marrow transplantation (allo-BMT) after myeloablative conditioning, donor T cells received critical Delta-like1 (Dll1) and Delta-like4 (Dll4)-mediated Notch signals within the first 48 hours after transplant. The cellular niche providing Dll1/4 ligands was restricted to nonhematopoietic Ccl19-Cre$^+$ fibroblastic stromal cells rather than hematopoietic cells in secondary lymphoid organs (10). Additionally, both Ccl19-Cre$^+$ fibroblastic stromal cells (18) and CD11c$^+$ classical dendritic cells (19) have been shown to provide Dll4 signals to drive T follicular helper cell differentiation. These findings highlight fine spatial and temporal regulation of Notch signaling induction to mature T cells in these contexts. However, outside of these observations, little is known about when and where T cells receive Notch signals, and about the essential cellular sources of Notch ligands in a broader range of immune responses. Identifying a common specific and sensitive surface indicator of Notch signaling across different activated T cell subsets and immunologic contexts would aid in answering these important questions.

CD43 (sialophorin, leukosialin) is a transmembrane sialomucin with an extensively O-glycosylated extracellular domain that is highly expressed on T cells (20). Dynamic regulation of glycosyltransferases during T cell development and activation results in the expression of two CD43 glycoforms (21). Mature naïve T cells express a 115 kDa glycoform

characterized by core-1 O-glycans capped by sialic acid. During T cell activation, upregulated expression of *Gcnt1* and its protein product the core-2 GlcNAc transferase-1 (C2GlcNAcT-I) occurs. In concert with reciprocal downregulation of *St3gal1,* which encodes the sialyltransferase that caps core-1 glycans, these changes generate an activation-associated 130 kDa glycoform of CD43 characterized by core-2 O-glycans (22). The switch from core-1 to core-2 O-glycosylation of surface glycoproteins, including CD43 and P-selectin glycoprotein ligand-1 (PSGL-1), increases the affinity of immune cells for P- and E-selectins, thus allowing initial rolling of activated (23) and memory T cell subsets (24, 25) on inflamed endothelium. Glycoform-specific antibodies to CD43 enable the detection of unique glycosylated forms of CD43, correlating with the overall O-glycosylation status of surface proteins. The mAb S11 recognizes CD43 regardless of glycosylation (20), while 1B11 specifically recognizes the core-2 activation-associated O-glycoform (22). Others have used core-2 O-glycoform CD43 reactivity to identify recently activated effector, as opposed to memory $CD8^+$ T cells in response to lymphocytic choriomeningitis virus (LCMV) infection (26). Furthermore, alloreactive T cells upregulate the core-2 O-glycoform of CD43, but not other glycoforms of CD43 during GVHD (27, 28). Regulation of *Gcnt1* expression and core-2 O-glycosylation, in turn, is context-dependent. Central memory $CD8^+$ T cells upregulate *Gcnt1* expression and subsequent CD43 core-2 O-glycoform reactivity in a TCR-independent but IL-15-dependent manner in vivo (24). In vitro studies have shown that naïve $CD4^+$ and $CD8^+$ T cells require TCR signals in cooperation with diverse cytokines, such as IL-2 and IL-12, to drive *Gcnt1* expression (29–31). However, IL-2 and IL-12 were dispensable in vivo for activated $CD8^+$ T cells (32). Thus, our understanding of the essential inputs that regulate *Gcnt1* expression and CD43 glycosylation remains limited.

Recently, we reported a transcriptional program activated by Notch signaling in alloantigen-specific $CD4^+$ T cells in a mouse model of allo-BMT and GVHD (33). Notch signaling was required for inflammatory cytokine production and lethal T cell alloreactivity (8, 10, 34). Interestingly, induction of *Gcnt1* mRNA depended on both alloantigenic stimulation and Notch signals. These findings suggested that core-2 O-glycosylation of CD43 and other surface proteins may serve as a new surface marker to indicate the receipt of functional Notch signals. To establish whether core-2 O-glycosylation of CD43 depended on Notch signals, we used flow cytometric analysis with glycoform-specific antibodies to CD43. Blockade of the Dll1/4 Notch ligands decreased the core-2 O-glycosylation of CD43 in a dose-dependent manner, while overall CD43 expression remained stable or even increased slightly. Regulation was cell-intrinsic, depended on canonical Notch signaling, and was observed across all recently activated T cell subsets. However, *Gcnt1*-deficient T cells with intact Notch still drove lethal GVHD, indicating that Notch signaling instructs a wider pathogenic program than core-2 O-glycosylation. Instead, core-2 O-glycosylation serves as a sensitive and simple flow cytometric indicator of Notch signaling in recently antigen-activated T cells. Core-2 O-glycosylation status successfully predicted whether T cells had received critical Notch signals in multiple models of allotransplantation, immunization, bacterial infection, and viral infection. Together these data show that Notch signals are critical to drive *Gcnt1*-dependent core-2 O-glycosylation in recently activated T cells, although *Gcnt1*-dependent core-2 O-glycosylation is not required for GVHD lethality. We propose that the core-2 O-glycoform of CD43 can be used as a simple flow cytometric

readout to map how Notch signaling regulates T cell activation, differentiation, and effector function, opening new avenues for a deeper understanding of Notch signaling's contribution to immune responses.

Methods

Mice.

C57BL/6 x BALB/c F1 (CBF1, H-$2^{b/d}$, Thy1.2), C57BL/6 (B6, H-$2^{b/b}$, Thy1.2), C57BL/6-Thy1.1/2 (B6, H-$2^{b/b}$, Thy1.1/2) mice were bred at the University of Michigan and the University of Pennsylvania. BALB/cJ mice were purchased from Jackson Laboratories. Mx1-Cre, Ccl19-Cre (35), CD4-Cre, *Dll1*$^{f/f}$, *Dll4*$^{f/f}$, *Notch1*$^{f/f}$, *Notch2*$^{f/f}$ and *ROSA26*^{DNMAMLf} alleles (abbreviated DNMAML) were described previously (8, 10). 4C *Rag1*$^{-/-}$TCR transgenic mice on the B6 background reactive to I-A^d were previously described (36). *Gcnt1*-deficient mice were previously described (37). OT-I TCR transgenic mice recognize the Ovalbumin (OVA) peptide SIINFEKL and were maintained on the B6 background. E8I-Cre^{+}*Notch1*$^{f/f}$ *Notch2*$^{f/f}$ lack *Notch1/2* genes in $CD8^+$ T cells, as described (2). For transplantation experiments, cohoused littermate controls were used for donors and recipients at the University of Michigan or the University of Pennsylvania, per protocols approved by the University of Pennsylvania's Office of Regulatory Affairs and the University of Michigan's Committee on Use and Care of Animals. For *Listeria monocytogenes* infection, experimental mice were housed at the Maisonneuve-Rosemont Hospital Research Center Facility, and treated in accordance with the Canadian Council on Animal Care guidelines.

Bone marrow transplantation, systemic Ab-mediated Notch inhibition, and GVHD assessment.

For transplantation, CBF1 recipients were irradiated using a Cesium-137 source with titrated doses: high-intensity myeloablative conditioning (11 Gy, split into two doses separated by 3h), reduced-intensity non-myeloablative conditioning (3 Gy), or no conditioning. Recipients were 8-16 weeks old. Both female and male mice were used as recipients and equally distributed among experimental groups. T cell-depleted bone marrow (TCD BM) prepared with anti-Thy1.2 antibodies and complement (Cedar Lane Laboratories) was injected i.v. with or without splenocytes and/or purified T cells, as described (9). Cell numbers infused for each experiment are noted in the text and figure legends. For experiments with 4C $CD4^+$ T cells, T cells were purified with negative magnetic selection for $CD4^+$ T cells (Stem Cell Technologies) and labeled with eFluor450 cell proliferation dye. For polyclonal experiments, wild-type, *Gcnt1*-deficient or dnMAML T cells were purified with negative magnetic selection for T cells (Stem Cell Technologies) and labeled with eFluor450 cell proliferation dye (Invitrogen). For long-term experiments, mice received noted doses of splenocytes and/or lymph node cells with TCD BM. Clinical GVHD scores and weight changes were monitored at least once weekly, as described (38). In selected experiments, recipient mice received humanized IgG1 mAbs specific for Dll1 or Dll4 (5 mg/kg i.p.) (9). A human IgG1 Ab to Herpes Simplex Virus gD glycoprotein was used as isotype control. Each antibody batch was tested for specificity and efficacy by assessing loss

of Dll4-dependent T cell progenitors (39) or Dll1-dependent marginal zone B cells in vivo (40).

Generation of BM hematopoietic chimeras.

Generation of BM chimeras was previously described (10). 8-12 week old CBF1 Mx1-Cre^{+} *Dll1*$^{f/f}$ *Dll4*$^{f/f}$ or Cre- littermate control donor mice received 5 i.p. injections of 50 μg poly(I:C) (Amersham) every other day. Two weeks after the last dose, bone marrow was harvested and transplanted into lethally irradiated (11 Gy) 8-12 week old CBF1 Ccl19-Cre^{+} *Dll1*$^{f/f}$ *Dll4*$^{f/f}$ or Cre- littermate controls. Mice were rested for 6 weeks to generate four-way chimeras lacking Dll1/4 genetically in the hematopoietic compartment, Ccl19-Cre^{+} fibroblastic compartment, both, or neither. Mice were then subjected to an infusion of 60 $\times 10^6$ lymph node cells from MHC-mismatched C57BL/6 mice.

BMDC generation, immunization, *Listeria monocytogenes* infection, chronic Lymphocytic Choriomeningitis Virus infection (LCMV clone 13), and analysis of T cell response.

Bone-marrow derived DCs were generated with GM-CSF and IL-4 as previously described (2), matured with LPS (100 ng/mL; Sigma) plus the TLR7/8 agonist R848 (100 ng/mL; Sigma) and loaded with $OVA_{257\text{-}264}$ peptide (SIINFEKL, 2 μg/mL; Sigma). A total of 5×10^5 DCs were i.v. injected. For experiments with OT-I cells, 5×10^4 purified (Stem Cell Technologies) CD45.1^{+} OT-I CD8^{+} T cells were adoptively transferred on the day before DC immunization. To assay anti-infectious responses, *L. monocytogenes* expressing ovalbumin (Lm-OVA) was grown, as described (2). A sublethal dose of 2×10^3 CFUs was i.v. injected. The endogenous CD8^{+} T cell response was monitored with K^{b}-OVA staining. To monitor response to chronic viral infection, mice were infected with LCMV clone 13 (2×10^6 PFU i.v.) and virus-specific CD8^{+} T cells were assayed at day 8 and day 30 post-infection with K^{b}-gp33 tetramer staining.

In vitro 4C CD4^{+} T cell stimulation on OP9 stroma.

OP9 cell lines overexpressing Dll1 and Dll4 have been described before (41, 42). The night before the experiment, 1×10^4 OP9 cells were seeded onto 96-well flat-bottom plates in 20% FCS + αMEM. 4C wild-type CD4^{+} T cells and 4C dnMAML CD4^{+} T cells were purified, labeled with eFluor450 proliferation dye and plated in a ratio of 2:2:1 with BMDCs from poly(I:C)-induced Mx1-Cre$^{+/-}$ *Dll1*$^{f/f}$ *Dll4*$^{f/f}$ CBF1 mice in complete RPMI (10% FCS) + 2β-mercaptoethanol. Blocking antibodies (anti-Dll1, anti-Dll4, both, or isotype control) were provided at a concentration of 25 μg/mL. Cells were harvested at day 4 post-plating.

Preparation of single-cell suspensions from lymphoid and GVHD target organs.

Single-cell suspensions of cells from spleen, mesenteric lymph node, or pooled peripheral lymph nodes (cervical, brachial, axial, inguinal) were prepared by physical disruption through 70 μm cell strainers. Single-cell suspensions were prepared from liver (12), intestinal lamina propria, and intestinal epithelium (8) as previously described.

Abs, flow cytometry, and cell sorting.

The following antibodies were from Biolegend: anti-CD4 (clone GK1.5); CD8α (clone 53-6.7); CD44 (clone IM7); CD25 (clone PC61); CD45.1 (clone A20); CD45.2 (clone 104); Thy1.1 (clone OX-7); Thy1.2 (clone 30-H12); H-2K^{b} (clone AF6-88.5); H-2K^{d} (clone SF1-1.1); IFNγ (clone XMG1.2); IL-17A (clone TC11-18H10.1); pan-CD43 (clone S11), core-2 O-glycosylation CD43 (clone 1B11); KLRG1 (clone 2F1); CD127/IL7Rα (clone A7R34). Anti-FoxP3 (clone FJK-16s) was from eBioscience. Anti-Vβ13 (clone MR12-3) was from BD Biosciences. SIINFEKL peptide loading on H-2K^{b} MHC and conjugation to PE was done as previously described (43). Non-viable cells were excluded from analysis with Zombie Aqua Fixable Viability Dye (Biolegend), or DAPI (Sigma-Aldrich). For intranuclear staining, FoxP3/Transcription Factor Staining Buffer (eBioscience) was used per manufacturer's protocol. Assessment of intracellular T cell cytokine production after short ex vivo stimulus was previously described (10). Flow cytometric analysis was performed using a 4-laser Fortessa (BD). Sorting of T cells was performed using a 4-laser FACSAria II/III (BD). Alloreactive 4C T cells were defined as Thy1.1^{+} CD4^{+}. Naïve OT-I CD8^{+} T cells (CD8^{+}CD44^{lo}) and day 3 OT-I effector CD8^{+} T cells (CD8^{+}CD45.2^{+}CD44^{hi}) were sorted on a BD FACSARIA II.

Quantitative real-time PCR.

Donor 4C Thy1.1^{+} CD4^{+} T cells were FACS purified directly into TRIzol Reagent (Invitrogen). Total RNA was extracted with phenol/chloroform and purified with RNeasy Micro Kit (QIAGEN). cDNA was generated with SuperScript II (Invitrogen) using poly-dT primers and subjected to quantitative PCR with TaqMan reagents (Applied Biosystems). Gene expression analysis was performed using the following primers: *Gcnt1* (Mm02010556_s1); *St3gal1* (Mm00501483_m1)*; Hprt* (Mm03024075_m1). Relative gene expression was determined using the ΔΔCt method, with normalization to *Hprt.*

Statistical analysis.

Sample size for in vivo mouse experiments was determined empirically based on prior experience of known effect sizes and variation and used to calculate power with "pwr" statistical package in R. All statistical tests were performed using Prism software (GraphPad Prism version 8). Unless otherwise noted, data with more than one group was analyzed for differences with one-way ANOVA or two-way ANOVA depending on the number of factors. If a factor significantly explained the variation of the data multiple comparisons between groups were made with Tukey's test assuming $\alpha = 0.05$ and adjusted p-values were reported. The multiple comparisons performed are represented in the figures by lines between groups. Data with only two groups were compared with an unpaired, 2-tailed Student's *t*-test. If variance between the two groups differed significantly by an F test, Welch's correction for *t*-tests was applied. Survival curves were compared using a log-rank (Mantel-Cox) test. Unless otherwise noted graphs were generated in GraphPad Prism and presented as mean +/− one standard deviation. Unless otherwise noted, adjusted p-values for comparisons were reported as *p<0.05, **p<0.01, ***p<0.001.

Results

Delta-like Notch signals drive *Gcnt1* expression and core-2 O-glycosylation of CD43 in alloreactive CD4$^+$ T cells.

Hallmarks and transcriptional consequences of Notch signaling have been investigated systematically in developing T cells and in T cell leukemia (44, 45), but only recently in mature T cells in the context of allo-BMT (33). To identify potential functional targets of Notch signals in antigen-activated T cells that can be used as indicators of Notch signaling, we built on our discovery that Notch signaling plays a critical role to drive T cell pathogenicity and GVHD after allo-BMT (8, 9, 11, 33, 34, 46). To capture the effects of Notch signaling specifically in alloantigen-reactive T cells, and not in bystander T cells, we studied the transcriptome of 4C CD4$^+$ TCR transgenic T cells transplanted in syngeneic or allogeneic mouse recipients, with or without blocking antibodies to Dlll/4 Notch ligands. In this model, 4C CD4$^+$ T cells are activated by the host MHC class II I-A^d alloantigen, while intact Dll11/4-mediated signaling is critical to drive lethal GVHD (33). Transcriptomic profiling showed that the expression of canonical Notch target genes such as *Hes1, Dtx1,* and *Il2ra* was downregulated with pharmacologic Delta-like ligand blockade (33) (Fig. 1A). Interestingly, upregulation of *Gcnt1* transcripts induced by allogeneic T cell activation was completely abrogated by Delta-like ligand blockade (33) (Fig. 1A). This was confirmed by qPCR validation in a separate experiment (Fig. 1B), indicating that increased *Gcnt1* mRNA expression required both alloantigenic stimulation and Notch signals. Conversely, Delta-like ligand blockade induced a trend for increased expression of *St3gal1,* which encodes the sialyltransferase that adds a terminal sialic acid cap on core-1 O-glycans, making them inaccessible for modification by core-2 glycosyltransferases (Supplemental Fig. 1A–B). Other core-2 GlcNAc transferases were not highly expressed in 4C alloreactive T cells (Supplemental Fig. 1C).

As others showed that *Gcnt1* expression is critical for core 2 O-glycosylation of CD43 (22), we hypothesized that Notch signals would regulate cell surface expression of the core-2 glycoform of CD43 in recently activated T cells. We used a pan-CD43 (S11) and a core 2 O-glycoform specific (1B11) anti-CD43 antibody (Fig. 1C) to evaluate if Notch signaling regulates core 2 O-glycosylation in 4C CD4$^+$ T cells after transplantation into lethally irradiated (11 Gy) CBF1 recipients (H-2$^{b/d}$). By flow cytometric analysis, the proportion of 4C CD4$^+$ T cells reactive with 1B11 decreased upon Dll1/4 inhibition in a dose-dependent manner (Fig. 1D–E). However, mean S11 reactivity, which reflects total CD43 levels, was not negatively affected by Notch blockade, instead increasing slightly with the highest dose of Dll1/4 inhibitors (Fig. 1F). This correlated with increased mRNA levels of *Spn,* the gene encoding CD43, with Notch blockade (Supplemental Fig. 1D). To correct for any overall changes in CD43 expression, the ratio of 1B11 to S11 reactivity was calculated in individual cells. The 1B11/S11 reactivity ratio was dependent on Delta-like Notch signaling (Fig. 1F–G). To test if this regulation depended on the transcriptional functions of Notch signaling, we transplanted CBF1 recipients with wild-type 4C cells or 4C cells expressing the pan-Notch inhibitor dnMAML, which blocks canonical RBPJk/MAML-dependent signaling downstream of all Notch ligands and receptors (47). Importantly 4C and 4C-dnMAML cells showed similar levels of alloantigen-specific activation as indicated by similar CD44 levels

(Supplemental Fig. 1E–F). However, 4C-dnMAML cells had decreased 1B11 reactivity (Fig. 1H) and 1B11/S11 ratios (Fig. 1I) down to levels barely higher than isotype control staining levels. In contrast, cell surface CD25 in 4C-dnMAML cells, while lower than in wild-type 4C cells, remained above isotype control staining levels (Fig. 1J–K). This is consistent with our transcriptional profiling showing that Notch blockade decreased, but did not eliminate all alloreactivity-induced *Il2ra* expression (Fig. 1A). To test which Delta-like ligand could drive 1B11 reactivity, we used an in vitro system where Notch ligands were provided by OP9 stromal cell lines expressing either Dll1 (OP9-DL1) or Dll4 (OP9-DL4). Co-cultured wild-type 4C and 4C-dnMAML T cells were plated at a 1:1 ratio on this stroma. Alloantigenic stimulus to 4C T cells was provided by bone marrow-derived dendritic cells (BMDCs) from CBF1 Mx-Cre^{+} *Dll1*$^{f/f}$*Dll4*$^{f/f}$ lacking Delta-like Notch ligands. When plated on either OP9-DL1 or OP9-DL4 stromal lines, wild-type 4C cells showed increased 1B11/S11 ratios, which was blocked by ligand-specific antibodies (Fig. 1L). Thus, in concert with alloantigenic stimulus, either Dll1 or Dll4 could drive core-2 O-glycosylation of CD43 in vitro. Altogether, measuring 1B11 or the 1B11/S11 reactivity ratio quantified Notch signaling intensity in T cells through a simple flow cytometry-based assay of cell surface glycoproteins.

Core-2 O-glycosylation of CD43 depends on cell-intrinsic canonical Notch signaling in multiple alloreactive polyclonal T cell subsets.

Next, we evaluated the abundance of CD43 core-2 O-glycoforms in multiple polyclonal donor-derived T cell subsets after allo-BMT with high-intensity conditioning (11 Gy). We transplanted 1×10^{6} T-cell depleted bone marrow (TCD BM) plus B6 (H2$^{b/b}$, Thy1.1/2) wild-type or B6-dnMAML T cells labeled with the eFluor450 cell proliferation dye into MHC-mismatched CBF1 (H2$^{b/d}$, Thy1.2) hosts (Fig. 2A). 1B11 reactivity in proliferated eFluor450 dilute CD4^{+} conventional T cells (Tconv) and Treg was significantly reduced among dnMAML T cell subsets from day 4 until day 14 post-transplant. 1B11 reactivity was also significantly reduced in dnMAML CD8^{+} T cells, but to a lesser extent than in CD4^{+} T cells. Maximum differences occurred on day 4, suggesting higher dependence on Notch signaling at early time points for core-2 glycosylation (Fig. 2A–B). Notch-dependent regulation of core-2 glycosylation was seen in both secondary lymphoid organs (Fig. 2C) where Notch signals are first received, but also in GVHD target tissues (Fig 2C). These signals were imprinted early during T cell activation, as a single dose of Dll1/4 blocking antibodies at the time of transplant was sufficient to prevent upregulation of 1B11 reactivity, but not when delayed to day 2 (Supplemental Fig. 2A–C). To establish if regulation of 1B11 reactivity by Notch was cell-intrinsic, we co-transplanted wild-type and *Notch1/2*-deficient T cells, or wild-type and dnMAML T cells into MHC-mismatched CBF1 recipients. Both wild-type and Notch-deficient T cells proliferated similarly post-transplant (Supplemental Fig. 2D–E), as shown previously (8, 9). However, compared to co-transplanted wild-type T cells, both *Notch1/2*-deficient and dnMAML T cells had significantly diminished 1B11 reactivity (Fig. 2D–E). Furthermore, 1B11 reactivity predicted the ability of proliferated wild-type CD4^{+} T cells to produce IL-17 and IFNγ (Fig. 2F) and the ability of CD8^{+} T cells to produce IFNγ (Fig. 2G). Thus, across allogeneic polyclonal T cell subsets, core-2 O-glycosylation of CD43 requires cell-intrinsic canonical Notch signals and identifies alloreactive T cells with high cytokine-producing potential.

Notch loss-of-function impacts core-2 O-glycosylation to a similar degree as *Gcnt1* deficiency, but Notch signaling can drive GVHD through *Gcnt1*-independent mechanisms.

Upregulated *Gcnt1* expression is critical for core-2 O-glycosylation of mucin-like glycoproteins including CD43, as well as other selectin ligands such as PSGL-1. In fact, core-2 modifications are required for PSGL-1 to bind P-selectins (48) and perhaps E-selectins (30, 49). Interestingly, P-selectin-deficient mice were protected from GVHD, but T cells from PSGL-1 deficient mice still caused GVHD (50). This suggests that core-2 O-glycosylation of other selectin ligands, such as CD43, may mediate trafficking of alloreactive T cells in GVHD target organs. Loss of Notch signaling also blunted trafficking of alloreactive T cells into target GVHD tissues including the intestinal lamina propria in a model of acute GVHD (8) and skin in a model of chronic GVHD (12). Since Notch signaling regulates *Gcnt1* expression and core-2 glycosylation of CD43 and likely other selectin ligands, we evaluated if *Gcnt1* expression mediated trafficking to target tissues or other pathogenic effects of Notch signaling in T cells during GVHD. To compare the impact of Notch inhibition and *Gcnt1* loss in T cells, we transplanted wild-type, dnMAML, or *Gcnt1*-deficient B6 T cells into CBF1 recipients. dnMAML $CD4^+$ Tconv phenocopied $Gcnt1^{-/-}$ T cells, while dnMAML Treg and $CD8^+$ T cells nearly fully phenocopied $Gcnt1^{-/-}$ T cells in terms of 1B11 reactivity and 1B11/S11 ratio after allo-BMT (Fig. 3A–B). These effects were seen both in lymphoid organs and in target organs including liver, GI epithelium and lamina propria (Supplemental Fig. 3A–B). Thus, Notch signals were the dominant input driving *Gcnt1* expression and core-2 O-glycosylation in this context. Consistent with previously published results, dnMAML $CD4^+$ (Fig. 3C) and $CD8^+$ (Fig. 3D) T cells had impaired accumulation in target tissues, but not lymphoid tissues. However, $Gcnt1^{-/-}$ T cells accumulated in similar numbers as wild-type T cells in both lymphoid organs and target tissues, except for the small intestine epithelium. Thus, while trafficking and/or accumulation of alloreactive T cells in liver or GI target tissues relies on Notch signals, these effects of Notch signaling are not driven by *Gcnt1* expression and core-2 O-glycosylation. Furthermore, the production of inflammatory cytokines was blunted in dnMAML but not $Gcnt1^{-/-}CD4^+$ (Fig. 3E, Supplemental Fig. 3C) and dnMAML but not $Gcnt1^{-/-}$ $CD8^+$ T cells (Fig. 3F, Supplemental Fig. 3D). $FoxP3^+$ Tregs were also significantly expanded among dnMAML but not $Gcnt1^{-/-}$ $CD4^+$ T cells (Supplemental Fig. 3E). Consistent with these results, $Gcnt1^{-/-}$ T cells transplanted into wild-type recipients mediated GVHD lethality and morbidity with similar if not increased kinetics as compared to wild-type T cells (Fig. 3G, solid lines). Notch appeared to drive GVHD pathogenicity independently of core-2 O-glycosylation, as mice receiving $Gcnt1^{-/-}$ T cells could be protected from GVHD by inactivating the *Dll1/4* ligand genes in $Ccl19\text{-}Cre^+$ host fibroblastic stromal cells (Fig. 3G, dotted lines), as shown previously with wild-type T cells (46). Together, these data show that Notch signals are crucial for *Gcnt1*-mediated core-2 O-glycosylation of CD43 in alloreactive T cell subsets. However, Notch can drive GVHD pathogenesis through mechanisms independent of *Gcnt1*.

Core-2 O-glycosylation of CD43 in T cells predicts the cellular source of Notch ligands that drive lethal T cell alloreactivity after allo-BMT with myeloablative and nonmyeloablative conditioning.

Because Notch signals were necessary for cell-intrinsic upregulation of 1B11 reactivity, we hypothesized that 1B11 reactivity could be used as a surrogate marker of Notch signaling in activated T cells. As a corollary, 1B11 reactivity should predict which cellular subset is the critical source of Notch ligands that drive lethal T cell alloreactivity across multiple allo-BMT models. We previously reported that in fully MHC-mismatched allogeneic BMT with prior myeloablative conditioning, nonhematopoietic lymphoid tissue fibroblastic stromal cells lineage traced by the Ccl19-Cre transgene provided the critical Dll1/4 ligands to drive GVHD (10). However, nothing is known about the source of Notch ligands that drive lethal alloimmunity after transplantation with reduced-intensity conditioning (51), a clinically relevant scenario. Indeed, radiation-sensitive hematopoietic cells, eliminated in myeloablative models, may provide a critical source of Notch ligands to drive lethal T cell alloreactivity. To test this question, we used a “parent into F1” model of allo-BMT where expression of parental alloantigens by the recipient causes tolerance to donor cells, allowing transplantation with titratable conditioning intensity (38). In a model with high-intensity irradiation-based conditioning (11 Gy), mice that received dnMAML T cells were protected from GVHD, similarly to recipient mice lacking *Dll1/4* in Ccl19-Cre^{+} fibroblastic stromal cells (Fig. 4A), in concordance with our previous results in a fully MHC-mismatched model (10). To test if 1B11 reactivity could predict this outcome, we co-transplanted wild-type and dnMAML T cells into Ccl19-Cre^{+} *Dll1*$^{f/f}$*Dll4*$^{f/f}$ or littermate control mice. Wild-type recipients showed striking differences between co-transplanted dnMAML and wild-type CD4^{+} Tconv in 1B11 expression and 1B11/S11 ratios (Fig. 4B). In contrast, these differences disappeared in Ccl19-Cre^{+} *Dll1*$^{f/f}$*Dll4*$^{f/f}$ recipients, indicating that no additional source of Notch ligands was available to CD4^{+} Tconv beyond the critical source in fibroblastic stromal cells (Fig. 4B–C). Alloreactive CD8^{+} T cells showed similar effects, with the vast majority of Notch inputs driving 1B11 reactivity from Ccl19-Cre^{+} cells (Fig. 4B–C). We next studied GVHD in a parent into F1 model with non-myeloablative irradiation-based conditioning (3 Gy). The differences in 1B11 reactivity and 1B11/S11 ratio of co-transplanted wild-type and dnMAML T cells indicated that Notch signals were received by wild-type T cells in wild-type recipients. However, in Ccl19-Cre^{+} *Dll1*$^{f/f}$*Dll4*$^{f/f}$ recipients, these differences in 1B11 reactivity disappeared, except for CD8^{+} T cells in skin draining peripheral lymph nodes (pLN) where minor differences in 1B11 expression remained (Fig. 4D–E), suggesting another source of Notch ligands available to CD8^{+} T cells in these lymphoid organs. Consistent with these flow cytometric results, Ccl19-Cre^{+} *Dll1*$^{f/f}$ *Dll4*$^{f/f}$ recipient mice were protected from lethal GVHD (Fig. 4F). Thus, even after allotransplantation with reduced-intensity conditioning, non-hematopoietic fibroblastic stromal cells were the critical source of Notch ligands that drive GVHD.

Core-2 O-glycosylation of donor T cells predicts a fibroblastic source of Notch ligands that drives lethal alloreactivity after donor lymphocyte infusion without prior conditioning.

In models with no prior conditioning, Notch also drives lethal alloimmunity, but the source of ligands remains unknown (8). To test the key cellular source of Notch ligands after allotransplantation with no prior conditioning, we created four-way bone marrow chimeric

recipient mice with loss of Delta-like ligands in different cellular compartments. Wild-type or Ccl19-Cre^{+} *Dll1*$^{f/f}$*Dll4*$^{f/f}$ CBF1 mice were transplanted after lethal irradiation with bone marrow from poly(I:C)-induced Mx-Cre^{+} *Dll1*$^{f/f}$*Dll4*$^{f/f}$ or *Cre*$^{-}$ control CBF1 mice. Chimeras were allowed to reconstitute for six weeks, generating recipients lacking Delta-like ligands in the hematopoietic compartment (Fig. 5A, **recipient ii**), fibroblastic stromal compartment **(recipient iii)**, both **(recipient iv)**, or neither **(recipient i)**. These mice then received a parental donor lymphocyte infusion of co-transferred 5×10^{6} wild-type and 5×10^{6} dnMAML B6 T cells ($H2^{b/b}$) without prior conditioning– a model capable of triggering alloimmune-mediated hematopoietic failure in CBF1 recipients ($H2^{b/d}$) (Fig. 5A). To predict the critical cellular source(s) of Notch signaling, we examined 1B11 and S11 reactivity in these co-transferred T cells (Fig. 5B–C) at day 6 post-infusion. Presence of Dll1/4 in the hematopoietic compartment had no impact on CD4^{+} Tconv Notch-dependent 1B11 reactivity (Fig. 5B–C, **recipient i vs. recipient ii**). However, loss of Dll1/4 ligands in the fibroblastic stromal compartment eliminated Notch-dependent 1B11 reactivity (Fig. 5B–C, **recipient i vs. recipient iii**). Alloreactive CD8^{+} T cells also depended on a fibroblastic source of Dll1/4 to show increased Notch-dependent 1B11 reactivity (Fig. 5D–E). Thus, we hypothesized that a fibroblastic source of Delta-like Notch ligands would be critical to drive lethal alloreactivity. To test this hypothesis, we transplanted CBF1 recipients with no prior conditioning and with 50^{6} lymph node cells from wild-type or dnMAML parental B6 mice. In this model, lethal T cell alloreactivity depended on canonical Notch signaling and was rescued when the fibroblastic stromal source of Dll1/4 was eliminated (Fig. 5F). Thus, 1B11 reactivity predicted the functionally relevant source of Notch ligands, and fibroblastic stromal cells remained the essential source even in the absence of irradiation conditioning.

Delta-like Notch signals drive core-2 O glycosylation of CD43 and CD8^{+} T cell effector differentiation after dendritic cell immunization.

To assess if Notch-dependent regulation of CD43 core-2 O-glycosylation applied to other types of antigen-activated T cells, we used a model of BMDC immunization pulsed with OVA peptide (DC-OVA). In this model, CD8^{+} T cell differentiation into KLRG1^{+}IL7R^{-} short-lived effector cells (SLECs) depends on cell-intrinsic Notch signals (2, 3). However, the generation of KLRG1^{-}IL7R^{-} early effector cells (EECs) and KLRG1^{-}IL7R^{+} memory precursor cells (MPECs) remains intact. At the time of adoptive DC-OVA transfer, mice were treated with anti-Dll1/4 or isotype control antibodies as noted in Fig. 6A. On day 10, Ag-specific CD8^{+} T cells were assessed by K^{b}-OVA tetramer staining (Fig. 6A). The overall percentage (Fig. 6A) and total number (not shown) of Ag-specific CD44^{+}CD8^{+} T cells were not affected by Dll1/4 blockade. However, differentiation into SLECs was blunted by anti-Dll1/4 antibodies (Fig. 6B). Consistent with the effects of Notch on core-2 O-glycosylation, 1B11 reactivity of OVA-specific CD8^{+} T cells depended on Dll1/4 Notch signals (Fig. 6C). The Notch-dependent 1B11 reactivity was not restricted to SLECs, but was also seen in OVA-specific CD8^{+} T cells MPECs and EECs, suggesting that these cellular subsets have also received Notch signals (Fig. 6D). Concordant results were observed when the response of adoptively transferred OT-I cells to DC-OVA was examined (Fig. 6E–G). These data show that Notch regulates short-lived effector cell differentiation and 1B11 reactivity in polyclonal and monoclonal models of OVA responsiveness.

Delta-like Notch signals control core-2 O-glycosylation of CD43 in Ag-specific CD8$^+$ T cells after *Listeria* infection.

Compared to infection, DC-OVA immunization does not induce robust innate immune stimuli. Thus, it is possible that additional cytokine pathways (such as IL-12) that have been shown to drive core-2 O-glycosylation in vitro (31) may not be triggered in this model. To determine if *Gcnt1* expression was also regulated by Notch during an anti-infectious response, we studied control vs. *Notch1/2*-deficient OT-I CD8$^+$ T cells in naïve mice and on day 3 after a sublethal dose of *Listeria monocytogenes* expressing ovalbumin (Lm-OVA). *Gcnt1* expression was induced after Lm-OVA infection in control, but not in Notch-deficient OT-I cells (Fig. 7A). Next, we administered Lm-OVA to wild-type or E8I-Cre$^+$ *Notch1*$^{f/f}$ *Notch2*$^{f/f}$ mice (lacking *Notch1/2* in all CD8$^+$ T cells). In parallel, we treated a group of wild-type mice with anti-Dll1/4 antibodies. Eliminating Notch signals either through loss of Notch1/2 receptors or through antibody-mediated Dll1/4 blockade did not impair or even slightly increased the overall expansion of antigen-specific CD8$^+$ T cells after Lm-OVA infection (Fig. 7B). However, differentiation into SLECs depended on CD8$^+$ T cell-intrinsic Notch signals, which was recapitulated by blocking Delta-like ligands (Fig. 7C). Consistently, 1B11 reactivity in bulk Ag-specific CD8$^+$ (Fig. 7D) and fractionated SLEC, EEC and MPEC subsets (Fig. 7E) depended on cell-intrinsic Notch signals and Delta-like Notch ligands (Fig. 7C–E). Compared to wild-type or E8I-Cre$^+$ *Notch1*$^{f/f}$ *Notch2*$^{f/f}$ mice, CD44$^+$CD4$^+$ T cells from mice receiving anti-Dll1/4 treatment had decreased 1B11 reactivity, indicating that Notch also regulates core-2 O-glycosylation in activated CD4$^+$ T cells after Lm-OVA infection (Fig. 7F). Furthermore, 1B11 reactivity was higher in wild type compared to E8I-Cre$^+$ *Notch1*$^{f/f}$*Notch2*$^{f/f}$ mice at day 8 and day 30 after LCMV clone 13 infection (Supplemental Fig. 4). Altogether, our data identify core-2 O-glycosylation and 1B11 reactivity as conserved and sensitive readouts of Notch signaling activity in T cells in multiple types of T cell responses.

Discussion

Multiple studies have shown that Notch signals regulate T cell differentiation and function during adaptive immune responses with context-specific effects. However, in most contexts, little is known about the cellular source, regulation, and timing of Notch signals received by T cells. Identification of a simple and generalizable cell surface marker of Notch signaling in activated T cell subsets will enhance our understanding of how Notch shapes T cell responses in specific immune contexts.

In this study, we report that *Gcnt1*-dependent core-2 O-glycosylation of CD43 behaves as a new cell surface marker to indicate whether a T cell has received Notch signals after antigen activation. This marker was quantitative, as it directly correlated to dose-dependent pharmacologic blockade of Notch ligands and could be easily monitored by flow cytometry with the mAb 1B11. Upregulated core-2 O-glycosylation of CD43 was cell-intrinsically controlled by Notch signaling within multiple T cell subsets and depended on Notch signals mediated via its canonical transcriptional activation complex. Importantly, the usefulness of this new surface marker was generalizable from alloimmunity to immunization, bacterial,

and viral infection models. Furthermore, monitoring CD43 glycosylation status could predict the critical cellular sources of Notch ligands that drove lethal alloimmunity.

We and others previously relied on CD25 as a marker of Notch signaling, as its expression is regulated by Notch in developing as well as mature T cells (52). However, 1B11 functioned as a superior marker for Notch signaling over CD25 for three reasons. First, blocking Notch signaling after allo-BMT expanded the proportion of FoxP3$^+$ Tregs, which highly express CD25 irrespectively of Notch signals (8, 11). Instead, 1B11 reactivity in Tregs was regulated by Notch, as it was in Foxp3$^-$CD4$^+$ conventional T cells. Second, 1B11 reactivity appears more sensitive and less transient than CD25 expression. For example, we had previously not observed decreased CD25 expression among dnMAML T cells in unirradiated allotransplantation models (8). Furthermore, only a small fraction of Ag-specific CD8$^+$ T cells express CD25 at day 8 post-infection (26) or day 6 post-DC immunization (53). Instead, we have shown that 1B11 remains highly detectable on CD8$^+$ T cells until day 14 post activation in transplantation, while others have shown its presence until at least day 14 after acute viral infection (26). In fact, virus-specific Notch-deficient CD8$^+$ T cells still had reduced 1B11 reactivity at day 30 after inoculation with LCMV clone 13, a model of chronic infection. Third, 1B11 reactivity had a stricter requirement for Notch signals than CD25, as we observed small but significant CD25 upregulation in dnMAML 4C T cells. Thus, 1B11 reactivity provides both more sensitive and more specific information than CD25 expression as a readout of Notch signaling activity.

In addition to its increased expression in GVHD (28, 54), 1B11 reactivity has previously been proposed as a marker to distinguish CD8$^+$ effector T cells from memory T cells in response to viral infection (26). Similar to our studies where high 1B11 reactivity correlated with cytokine production, the authors showed that high 1B11 reactivity correlated with cytolytic function. Because of the centrality of Notch signaling in driving CD8$^+$ T cell effector differentiation and short-lived effector functions, we speculate that Notch orchestrates both *Gcnt1*-dependent 1B11 reactivity and effector T cell differentiation during early stages of T cell activation. Whether other signals can bypass Notch signaling to drive activation-associated *Gcnt1* upregulation, core-2 O-glycosylation, and effector T cell differentiation remains to be seen. In contrast to in vitro experiments, in vivo findings showed that IL-12, IL-2, and IL-15 were dispensable for functional P-selectin ligand formation and thus likely for *Gcnt1* induction and core-2 O-glycosylation in effector CD8$^+$ T cells (23). In CD4$^+$ T cells, *Gcnt1* expression depended on TCR signaling in concert with STAT4-dependent IL-12 signaling or other diverse cytokines in vitro (29, 31). However, little was known about the regulation of *Gcnt1* in CD4$^+$ T cells in vivo. Given that dnMAML CD4 Tconv fully recapitulated and dnMAML CD8 T cells largely recapitulated the impact of *Gcnt1* deficiency on 1B11 expression, Notch signals are critical for *Gcnt1* upregulation and core-2 O-glycosylation at least in the context of allo-BMT. We show that a short pulse of Notch signaling in cooperation with antigen activation drives 1B11 reactivity in effector T cells. Over time, 1B11 reactivity tends to decay in antigen-activated CD4$^+$ and CD8$^+$ T cells. In contrast, memory CD8$^+$ T cells were reported to express *Gcnt1* in an IL-15-dependent and antigen-independent manner (24). It would be interesting to test if Notch signals also cooperate with IL-15 in this context to regulate *Gcnt1* expression.

To show the utility of 1B11 reactivity as a surrogate surface marker of Notch signaling, we asked whether it could be used to predict the cellular source of Notch ligands that drive lethal alloimmunity. We previously showed that non-hematopoietic fibroblastic stromal cells lineage traced by the Ccl19-Cre transgene were the source of Delta-ligands after allo-BMT with high-intensity myeloablative conditioning (46). However, in models of allotransplantation with reduced or no prior conditioning, it was unclear if viable hematopoietic cells could substitute for fibroblastic stromal cells as a source of Notch ligands. By comparing 1B11 reactivity in co-transferred wild-type and dnMAML T cells, we predicted that in both models of allotransplantation with reduced or no prior conditioning, fibroblastic stromal cells were necessary and hematopoietic cells dispensable to drive lethal Notch-mediated T cell pathogenicity. Additionally, we used 1B11 reactivity as a surrogate marker to compare Notch signals received by $CD8^+$ T cells during *L. monocytogenes* infection. Using 1B11, we predicted that pharmacologic blockade of Dll1/4 ligands would recapitulate cell-intrinsic loss of Notch1/2 receptors in $CD8^+$ T cells. This was confirmed when studying the differentiation of Ag-specific $CD8^+$ T cells into SLECs. Together, these findings show for the first time that Delta-like Notch ligands are essential and Jagged ligands are dispensable during Notch-dependent $CD8^+$ T cell differentiation. This is consistent with recent findings that dendritic cells lacking Dll1 but not Jag1 had decreased ability to support anti-tumor T cell response (55). Furthermore, the fact that pharmacologic blockade of Dll1/4 ligands fully recapitulated the loss of 1B11 reactivity and effector differentiation seen in Notch1/2-deficient $CD8^+$ T cells suggests there is a limited role for ligand-independent Notch signaling in vivo, in contrast to suggestions by other groups based on in vitro findings (56, 57).

What is the functional significance of Notch-dependent *Gcnt1*-mediated core-2 O-glycosylation in activated T cell subsets during GVHD? *Gcnt1* is crucial for the creation of functional ligands for P- and E-selectin in leukocytes and their trafficking into some inflamed non-lymphoid tissues. In our model of MHC-mismatched allo-BMT, *Gcnt1*-deficient T cells could still traffic into liver and GI target tissues and mediate lethal GVHD in a Notch-dependent manner. Thus, *Gcnt1* function is likely not central to T cell pathogenicity in this context. Interestingly, others have shown that P-selectin-deficient recipients had decreased lethality in GVHD models, although PSGL1-deficient T cells did not induce reduced mortality (50). Together with our data, these findings suggest that T cells can traffic into the GI tract and liver independently of functional P-selectin ligands. Other mechanisms such as $\alpha 4\beta 7$/MAdCAM-1 interactions may also be involved in T cell trafficking into the gut during GVHD (58). P-selectin-deficient mice may be protected from GVHD as subsequent migration of donor bone marrow-derived myeloid cells into target tissues, which is necessary to sustain GVHD (59, 60), may require P-selectin to traffic into target tissues. Additionally, because morbidity in our allo-BMT model is predominantly driven by early GI damage, we did not examine skin-homing T cells, which may have a more stringent requirement for expression of P- and E-selectin ligands. In fact, we recently showed in a model of chronic GVHD that Notch-deprived T cells had significantly impaired accumulation in the skin (12).

In humans, a core-2 O-glycan-specific mAb for CD43, 1D4, recognizes a subset of what has been described as memory $CD4^+CD45RO^+$ mature T cells (61). Another mAb, T305,

specific for core-2 O-glycosylated CD43 showed increased reactivity in T cells of patients with GVHD, autoimmunity or viral infection (62). These findings suggest that similar regulation of core-2 O-glycans may exist in recently activated human effector T cells in humans.

Much remains to be understood about Notch signaling during T cell activation. Our work defining a cell-intrinsic generalizable indicator of Notch signals in activated T cell subsets will help answer pressing questions in the field. For example, the cellular source of Notch ligands remains unknown in immunization and infection models. Also, little is known about the dynamic regulation of Notch ligand expression and activity in antigen-presenting cells vs. fibroblastic stromal cells. Assessing surface core-2 O-glycosylation of CD43, a simple marker correlated to Notch-dependent T cell function, will help decipher the immunobiology of Notch signaling in T cell immunity.

Supplementary Material

Refer to Web version on PubMed Central for supplementary material.

Acknowledgments

Supported by: National Institute of Allergy and Infectious Diseases (NIAID; R01-AI091627, to IM and R37-AI34495 to BRB), Canadian Institutes of Health Research (CIHR; PJT-14903 and PJT-152988 to NL), National Heart, Lung, and Blood Institute (NHLBI; R01-HL118979 and R01-HL056067, to BRB), T32-GM007863 from NIGMS and F30-AI136325 from NIAID (to EP).

Disclosures: BRB receives remuneration as an advisor to Kamon Pharmaceuticals Inc, Five Prime Therapeutics Inc, Regeneron Pharmaceuticals, Magenta Therapeutics and BlueRock Therapeutics, as well as research support from Fate Therapeutics, RXi Pharmaceuticals, Alpine Immune Sciences Inc, Abbvie Inc., BlueRock Therapeutics, Leukemia and Lymphoma Society, Childrens' Cancer Research Fund, KidsFirst Fund. He is a co-founder of Tmunity.

References

1. Vijayaraghavan J, and Osborne BA. 2018 Notch and T Cell Function – A Complex Tale. Adv. Exp. Med. Biol 1066: 339–354. [PubMed: 30030835]
2. Mathieu M, Duval F, Daudelin J-F, and Labrecque N. 2014 The Notch Signaling Pathway Controls Short-Lived Effector CD8+ T Cell Differentiation but Is Dispensable for Memory Generation. J. Immunol 194: 5654–62.
3. Backer R a, Helbig C, Gentek R, Kent A, Laidlaw BJ, Dominguez CX, de Souza YS, van Trierum SE, van Beek R, Rimmelzwaan GF, ten Brinke A, Willemsen a M., van Kampen AHC, Kaech SM, Blander JM, van Gisbergen K, and Amsen D. 2014 A central role for Notch in effector CD8+ T cell differentiation. Nat. Immunol 15: 1143–1151. [PubMed: 25344724]
4. Neal LM, Qiu Y, Chung J, Xing E, Cho W, Malachowski AN, Sandy-Sloat AR, Osterholzer JJ, Maillard I, and Olszewski MA. 2017 T Cell–Restricted Notch Signaling Contributes to Pulmonary Th1 and Th2 Immunity during Cryptococcus neoformans Infection. J. Immunol 199: 643–655. [PubMed: 28615417]
5. Auderset F, Schuster S, Coutaz M, Koch U, Desgranges F, Merck E, MacDonald HR, Radtke F, and Tacchini-Cottier F. 2012 Redundant Notch1 and Notch2 signaling is necessary for IFNγ secretion by T helper 1 cells during infection with Leishmania major. PLoS Pathog. 8: e1002560. [PubMed: 22396647]
6. Sugimoto K, Maekawa Y, Kitamura A, Nishida J, Koyanagi A, Yagita H, Kojima H, Chiba S, Shimada M, and Yasutomo K. 2010 Notch2 signaling is required for potent antitumor immunity in vivo. J. Immunol 184: 4673–8. [PubMed: 20351182]

7. Sierra RA, Thevenot P, Raber PL, Cui Y, Parsons C, Ochoa AC, Trillo-Tinoco J, Del Valle L, and Rodriguez PC. 2014 Rescue of Notch-1 Signaling in Antigen-Specific CD8+ T Cells Overcomes Tumor-Induced T-cell Suppression and Enhances Immunotherapy in Cancer. Cancer Immunol. Res 2: 800–811. [PubMed: 24830414]
8. Zhang Y, Sandy AR, Wang J, Radojcic V, Shan GT, Tran IT, Friedman A, Kato K, He S, Cui S, Hexner E, Frank DM, Emerson SG, Pear WS, and Maillard I. 2011 Notch signaling is a critical regulator of allogeneic CD4+ T-cell responses mediating graft-versus-host disease. Blood 117: 299–308. [PubMed: 20870902]
9. Tran IT, Sandy AR, Carulli AJ, Ebens C, Chung J, Shan GT, Radojcic V, Friedman A, Gridley T, Shelton A, Reddy P, Samuelson LC, Yan M, Siebel CW, and Maillard I. 2013 Blockade of individual Notch ligands and receptors controls graft-versus-host disease. J. Clin. Invest 123: 1590–1604. [PubMed: 23454750]
10. Chung J, Ebens CLCL, Perkey E, Radojcic V, Koch U, Scarpellino L, Tong A, Allen F, Wood S, Feng J, Friedman A, Granadier D, Tran ITIT, Chai Q, Onder L, Yan M, Reddy P, Blazar BRBR, Huang AYAY, V Brennan TVT, Bishop DKK, Ludewig B, Siebel CWCW, Radtke F, Luther SASA, and Maillard I. 2017 Fibroblastic niches prime T cell alloimmunity through Delta-like Notch ligands. J. Clin. Invest 127: 1574–1588. [PubMed: 28319044]
11. Charbonnier L-M, Wang S, Georgiev P, Sefik E, and Chatila TA. 2015 Control of peripheral tolerance by regulatory T cell–intrinsic Notch signaling. Nat. Immunol 16: 1162–1173. [PubMed: 26437242]
12. Radojcic V, Paz K, Chung J, Du J, Perkey ET, Flynn R, Ivcevic S, Zaiken M, Friedman A, Yan M, Pletneva MA, Sarantopoulos S, Siebel CW, Blazar BR, and Maillard I. 2018 Notch signaling mediated by Delta-like ligands 1 and 4 controls the pathogenesis of chronic GVHD in mice. Blood 132: 2188–2200. [PubMed: 30181175]
13. Wood S, Feng J, Chung J, Radojcic V, Sandy-Sloat AR, Friedman A, Shelton A, Yan M, Siebel CW, Bishop DK, and Maillard I. 2015 Transient blockade of delta-like Notch ligands prevents allograft rejection mediated by cellular and humoral mechanisms in a mouse model of heart transplantation. J. Immunol 194: 2899–2908. [PubMed: 25687759]
14. Riella LV, Ueno T, Batal I, De Serres SA, Bassil R, Elyaman W, Yagita H, Medina-Pestana JO, Chandraker A, and Najafian N. 2011 Blockade of Notch Ligand Delta1 Promotes Allograft Survival by Inhibiting Alloreactive Th1 Cells and Cytotoxic T Cell Generation. J. Immunol 187: 4629–4638. [PubMed: 21949024]
15. Magee CN, Murakami N, Borges TJ, Shimizu T, Safa K, Ohori S, Cai S, Uffing A, Azzi J, Elyaman W, Charbonnier L-M, Liu K, Toprak D, Visner G, Chatila TA, Siebel CW, Najafian N, and Riella LV. 2019 Notch-1 Inhibition Promotes Immune Regulation in Transplantation via Treg-Dependent Mechanisms. Circulation. 140(10):846–863. [PubMed: 31266349]
16. Sandy AR, Stoolman J, Malott K, Pongtornpipat P, Segal BM, and Maillard I. 2013 Notch signaling regulates T cell accumulation and function in the central nervous system during experimental autoimmune encephalomyelitis. J. Immunol 191: 1606–1613. [PubMed: 23825310]
17. Minter L, Turley D, Das P, Shin HM, Joshi I, Lawlor RG, Cho OH, Palaga T, Gottipati S, Telfer JC, Kostura L, Fauq AH, Simpson K, Such KA, Miele L, Golde TE, Miller SD, and Osborne BA. 2005 Inhibitors of γ-secretase block in vivo and in vitro T helper type 1 polarization by preventing Notch upregulation of Tbx21. Nature Immunol. 8: 680–688
18. Fasnacht N, Huang H-Y, Koch U, Favre S, Auderset F, Chai Q, Onder L, Kallert S, Pinschewer DD, MacDonald HR, Tacchini-Cottier F, Ludewig B, Luther SA, and Radtke F. 2014 Specific fibroblastic niches in secondary lymphoid organs orchestrate distinct Notch-regulated immune responses. J. Exp. Med 211: 2265–2279. [PubMed: 25311507]
19. Dell'Aringa M, and Reinhardt RL. 2018 Notch signaling represents an important checkpoint between follicular T-helper and canonical T-helper 2 cell fate. Mucosal Immunol. 11: 1079–1091. [PubMed: 29467447]
20. Baecher-Allan C, Kemp J, Dorfman K, Barth R, and Frelinger J. 1993 Differential epitope expression of Ly-48 (mouse leukosialin). Immunogenetics 37: 183–192. [PubMed: 7678405]
21. Hobbs SJ, and Nolz JC. 2017 Regulation of T Cell Trafficking by Enzymatic Synthesis of O-Glycans. Front. Immunol 8: 600. [PubMed: 28596771]

22. Barran P, Fellinger W, Warren CE, Dennis JW, and Ziltener HJ. 1997 Modification of CD43 and other lymphocyte O-glycoproteins by core 2 N-acetylglucosaminyltransferase. Glycobiology 7: 129–136. [PubMed: 9061371]

23. Carlow DA, Williams MJ, and Ziltener HJ. 2005 Inducing P-Selectin Ligand Formation in CD8 T Cells: IL-2 and IL-12 Are Active In Vitro but Not Required In Vivo. J. Immunol 174: 3959–3966. [PubMed: 15778352]

24. Nolz JC, and Harty JT. 2014 IL-15 regulates memory CD8+ T cell O-glycan synthesis and affects trafficking. J. Clin. Invest 124: 1013–1026. [PubMed: 24509081]

25. Osborn JF, Mooster JL, Hobbs SJ, Munks MW, Barry C, Harty JT, Hill AB, and Nolz JC. 2017 Enzymatic synthesis of core 2 O-glycans governs the tissue-trafficking potential of memory CD8 + T cells. Sci. Immunol 2(16).

26. Harrington LE, Galvan M, Baum LG, Altman JD, and Ahmed R. 2000 Differentiating between memory and effector CD8 T cells by altered expression of cell surface O-glycans. J. Exp. Med 191: 1241–1246. [PubMed: 10748241]

27. Ellies LG, Jones AT, Williams MJ, and Ziltener HJ. 1994 Differential Regulation of Cd43 Glycoforms on Cd4(+) and Cd8(+) T-Lymphocytes in Graft-Versus-Host Disease. Glycobiology 4: 885–893. [PubMed: 7537557]

28. Bagřiaçik EÜ, Armstrong MD, Okabe M, and Klein JR. 1999 Differential expression of CD43 isoforms on murine T cells and their relationship to acute intestinal graft versus host disease: studies using enhanced-green fluorescent protein transgenic mice. Int. Immunol 11: 1651–1662. [PubMed: 10508183]

29. Kansas GS, Ebel ME, Awe O, and Kaplan MH. 2015 MAPK α Cells via p38 T Selectin Ligand Expression on Murine CD4 Diverse Inflammatory Cytokines Induce. J Immunol 194: 5781–5788. [PubMed: 25941329]

30. Snapp KR, Heitzig CE, Ellies LG, Marth JD, and Kansas GS. 2001 Differential requirements for the O-linked branching enzyme core 2 1–6-N-glucosaminyltransferase in biosynthesis of ligands for E-selectin and P-selectin. Blood. 97(12):3806–3811. [PubMed: 11389020]

31. Lim YC, Xie H, Come CE, Alexander SI, Grusby MJ, Lichtman AH, and Luscinskas FW. 2001 IL-12, STAT4-dependent up-regulation of CD4(+) T cell core 2 beta-1,6-n-acetylglucosaminyltransferase, an enzyme essential for biosynthesis of P-selectin ligands. J. Immunol 167: 4476–4484. [PubMed: 11591774]

32. Carlow DA, Williams MJ, and Ziltener HJ. 2005 Inducing P-selectin ligand formation in CD8 T cells: IL-2 and IL-12 are active in vitro but not required in vivo. J. Immunol 174: 3959–3966. [PubMed: 15778352]

33. Chung J, Radojcic V, Perkey E, Parnell TJ, Niknafs Y, Jin X, Friedman A, Labrecque N, Blazar BR, V Brennan T, Siebel CW, and Maillard I. 2019 Early Notch Signals Induce a Pathogenic Molecular Signature during Priming of Alloantigen-Specific Conventional CD4+ T Cells in Graft-versus-Host Disease. J. Immunol 203: 557–568. [PubMed: 31182480]

34. Sandy AR, Chung J, Toubai T, Shan GT, Tran IT, Friedman a, Blackwell TS, Reddy P, King PD, and Maillard I. 2013 T cell-specific notch inhibition blocks graft-versus-host disease by inducing a hyporesponsive program in alloreactive CD4+ and CD8+ T cells. J. Immunol 190: 5818–5828. [PubMed: 23636056]

35. Chai Q, Onder L, Scandella E, Gil-Cruz C, Perez-Shibayama C, Cupovic J, Danuser R, Sparwasser T, Luther S, Thiel V, Rülicke T, Stein J, Hehlgans T, and Ludewig B. 2013 Maturation of Lymph Node Fibroblastic Reticular Cells from Myofibroblastic Precursors Is Critical for Antiviral Immunity. Immunity 38: 1013–1024. [PubMed: 23623380]

36. Brennan TV, Hoang V, Garrod KR, Liu F-C, Hayden T, Kim J, and Kang S-M. 2008 A new T-cell receptor transgenic model of the CD4+ direct pathway: level of priming determines acute versus chronic rejection. Transplantation 85: 247–255. [PubMed: 18212630]

37. Ellies LG, Tsuboi S, Petryniak B, Lowe JB, Fukuda M, and Marth JD. 1998 Core 2 Oligosaccharide Biosynthesis Distinguishes between Selectin Ligands Essential for Leukocyte Homing and Inflammation. Immunity 9: 881–890. [PubMed: 9881978]

38. Hill GR, Crawford JM, Cooke KR, Brinson YS, Pan L, and Ferrara JL. 1997 Total body irradiation and acute graft-versus-host disease: the role of gastrointestinal damage and inflammatory cytokines. Blood 90: 3204–3213. [PubMed: 9376604]
39. Hozumi K, Mailhos C, Negishi N, Hirano K, Yahata T, Ando K, Zuklys S, Holländer GA, Shima DT, and Habu S. 2008 Delta-like 4 is indispensable in thymic environment specific for T cell development. J. Exp. Med 205: 2507–2513. [PubMed: 18824583]
40. Hozumi K, Negishi N, Suzuki D, Abe N, Sotomaru Y, Tamaoki N, Mailhos C, Ish-Horowicz D, Habu S, and Owen MJ. 2004 Delta-like 1 is necessary for the generation of marginal zone B cells but not T cells in vivo. Nat. Immunol 5: 638–644. [PubMed: 15146182]
41. Schmitt TM, and Zúñiga-Pflücker JC. 2002 Induction of T cell development from hematopoietic progenitor cells by delta-like-1 in vitro. Immunity 17: 749–756. [PubMed: 12479821]
42. Schmitt TM, and Zúñiga-Pflücker JC. 2006 T-cell development, doing it in a dish. Immunol. Rev 209: 95–102. [PubMed: 16448536]
43. Lacombe MH, Hardy MP, Rooney J, and Labrecque N. 2005 IL-7 receptor expression levels do not identify CD8+ memory T lymphocyte precursors following peptide immunization. J. Immunol 175: 4400–4407. [PubMed: 16177081]
44. Weng AP, Ferrando AA, Lee W, Morris JP, Silverman LB, Sanchez-Irizarry C, Blacklow SC, Look AT, and Aster JC. 2004 Activating mutations of NOTCH1 in human T cell acute lymphoblastic leukemia. Science 306: 269–71. [PubMed: 15472075]
45. Wang H, Zou J, Zhao B, Johannsen E, Ashworth T, Wong H, Pear WS, Schug J, Blacklow SC, Arnett KL, Bernstein BE, Kieff E, and Aster JC. 2011 Genome-wide analysis reveals conserved and divergent features of Notch1/RBPJ binding in human and murine T-lymphoblastic leukemia cells. Proc. Natl. Acad. Sci 108: 14908–14913. [PubMed: 21737748]
46. Chung J, Ebens CL, Perkey E, Radojcic V, Koch U, Scarpellino L, Tong A, Allen F, Wood S, Feng J, Friedman A, Granadier D, Tran IT, Chai Q, Onder L, Yan M, Reddy P, Blazar BR, Huang AY, Brennan TV, Bishop DK, Ludewig B, Siebel CW, Radtke F, Luther SA, and Maillard I. 2017 Fibroblastic niches prime T cell alloimmunity through Delta-like Notch ligands. J. Clin. Invest 127: 1574–1588. [PubMed: 28319044]
47. Maillard I, Weng AP, Carpenter AC, Rodriguez CG, Sai H, Xu L, Allman D, Aster JC, and Pear WS. 2004 Mastermind critically regulates Notch-mediated lymphoid cell fate decisions. 104: 1696–1702.
48. Kumar R, Camphausen RT, Sullivan FX, Cumming DA. 1996 Core2 beta-1, 6-N-acetylglucosaminyltransferase enzyme activity is critical for P-selectin glycoprotein ligand-1 binding to P-selectin. Blood. 88(10):3872–3879. [PubMed: 8916952]
49. Li F, Wilkins PP, Crawley S, Weinstein J, Cummings RD, and McEver RP. 1996 Post-translational modifications of recombinant P-selectin glycoprotein ligand-1 required for binding to P- and E-selectin. J. Biol. Chem 271: 3255–3264. [PubMed: 8621728]
50. Lu SX, Holland AM, Na I-K, Terwey TH, Alpdogan O, Bautista JL, Smith OM, Suh D, King C, Kochman A, Hubbard VM, Rao UK, Yim N, Liu C, Laga AC, Murphy G, Jenq RR, Zakrzewski JL, Penack O, Dykstra L, Bampoe K, Perez L, Furie B, Furie B, and van den Brink MRM. 2010 Absence of P-selectin in recipients of allogeneic bone marrow transplantation ameliorates experimental graft-versus-host disease. J. Immunol 185: 1912–1919. [PubMed: 20622117]
51. Roderick JE, Gonzalez-Perez G, Kuksin CA, Dongre A, Roberts ER, Srinivasan J, Andrzejewski C, Fauq AH, Golde TE, Miele L, and Minter LM. 2013 Therapeutic targeting of NOTCH signaling ameliorates immune-mediated bone marrow failure of aplastic anemia. J. Exp. Med 210: 1311–1329. [PubMed: 23733784]
52. Adler SH, Chiffoleau E, Xu L, Dalton NM, Burg JM, Wells AD, Wolfe MS, Turka LA, and Pear WS. 2003 Notch signaling augments T cell responsiveness by enhancing CD25 expression. J. Immunol 171: 2896–2903. [PubMed: 12960312]
53. Boulet S, Daudelin J-F, and Labrecque N. 2014 IL-2 induction of Blimp-1 is a key in vivo signal for CD8+ short-lived effector T cell differentiation. J. Immunol 193: 1847–1854. [PubMed: 25015830]

54. Ellies LG, Jones AT, Williams MJ, and Ziltener HJ. 1994 Differential regulation of CD43 glycoforms on CD4 $^{+}$ and CD8 $^{+}$ T lymphocytes in graft-versus-host disease. Glycobiology 4: 885–893. [PubMed: 7537557]

55. Tchekneva EE, Goruganthu MUL, Uzhachenko RV, Thomas PL, Antonucci A, Chekneva I, Koenig M, Piao L, Akhter A, de Aquino MTP, Ranganathan P, Long N, Magliery T, Valujskikh A, Evans JV, Arasada RR, Massion PP, Carbone DP, Shanker A, and Dikov MM. 2019 Determinant roles of dendritic cell-expressed Notch Delta-like and Jagged ligands on anti-tumor T cell immunity. J. Immunother. Cancer 7: 95. [PubMed: 30940183]

56. Steinbuck MP, Arakcheeva K, and Winandy S. 2018 Novel TCR-Mediated Mechanisms of Notch Activation and Signaling. J. Immunol 200: 997–1007. [PubMed: 29288204]

57. Palaga T, Miele L, Golde TE, and Osborne BA. 2003 TCR-mediated Notch signaling regulates proliferation and IFN-gamma production in peripheral T cells. J. Immunol 171: 3019–3024. [PubMed: 12960327]

58. Fu Y-Y, Egorova A, Sobieski C, Kuttiyara J, Calafiore M, Takashima S, Clevers H, and Hanash AM. 2019 T Cell Recruitment to the Intestinal Stem Cell Compartment Drives Immune-Mediated Intestinal Damage after Allogeneic Transplantation. Immunity 51: 90–103 [PubMed: 31278057]

59. Koyama M, Cheong M, Markey KA, Gartlan KH, Kuns RD, Locke KR, Lineburg KE, Teal BE, Leveque-El Mouttie L, Bunting MD, Vuckovic S, Zhang P, Teng MWL, Varelias A, Tey S-K, Wockner LF, Engwerda CR, Smyth MJ, Belz GT, McColl SR, MacDonald KPA, and Hill GR. 2015 Donor colonic CD103+ dendritic cells determine the severity of acute graft-versus-host disease. J. Exp. Med 212: 1303–21. [PubMed: 26169940]

60. Matte CC, Liu J, Cormier J, Anderson BE, Athanasiadis I, Jain D, McNiff J, and Shlomchik WD. 2004 Donor APCs are required for maximal GVHD but not for GVL. Nat. Med 10: 987–992. [PubMed: 15286785]

61. Mukasa R, Homma T, Ohtsuki T, Hosono O, Souta A, Kitamura T, Fukuda M, Watanabe S, and Morimoto C. 1999 Core 2-containing O-glycans on CD43 are preferentially expressed in the memory subset of human CD4 T cells. Int. Immunol 11: 259–268. [PubMed: 10069424]

62. Fox RI, Hueniken M, Fong S, Behar S, Royston I, Singhal SK, and Thompson L. 1983 A novel cell surface antigen (T305) found in increased frequency on acute leukemia cells and in autoimmune disease states. J. Immunol 131: 762–767. [PubMed: 6602845]

Key Points

1. Notch signaling regulates *Gcnt1*-mediated core-2 O-glycosylation in activated T cells
2. The core-2 O-glycoform of CD43 reports Notch signals in multiple mouse T cell subsets

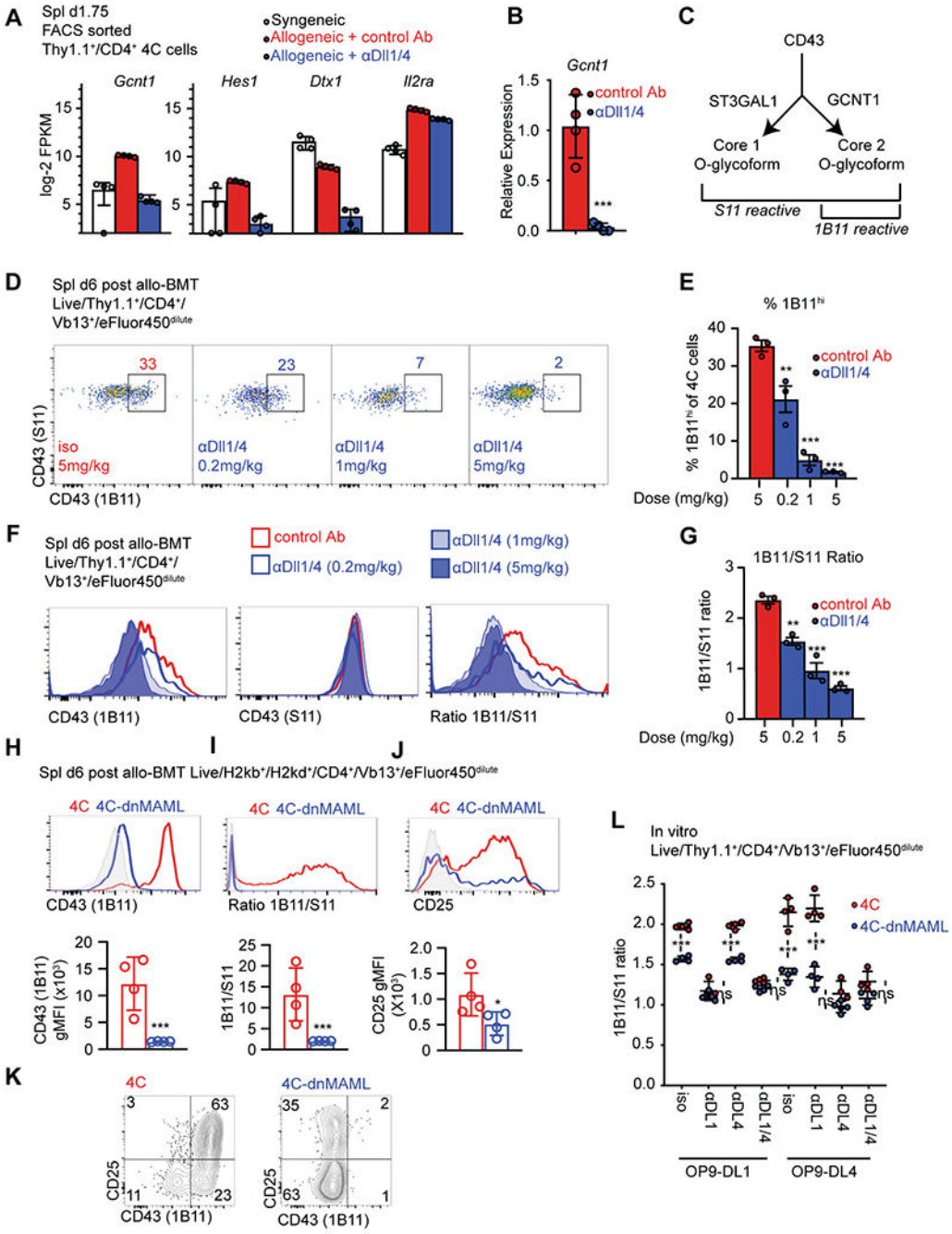

Figure 1. Notch signaling drives *Gcnt1*-mediated core-2 O-glycosylation of CD43 in alloreactive CD4$^+$ T cells.

(A-B) Purified I-A^b alloantigen-specific Vβ13$^+$ Thy1.1$^+$ 4C CD4$^+$ T cells were transplanted into lethally irradiated (11 Gy) B6 MHC-matched (syngeneic) or BALB/c MHC-mismatched (allogeneic) hosts with or without neutralizing antibodies to Delta-like1/4 (Dll1/4) Notch ligands, then sort purified at day 1.75 post-transplant. **(A)** Fragments per kilobase per million mapped reads (FPKM) for *Gcnt1* and highlighted Notch target gene transcripts from previously reported transcriptional profiling and **(B)** qRT-PCR validation of

Gcnt1 mRNA abundance from a separate experiment. **(C)** *Gcnt1* drives core-2 O-glycosylation of CD43 which can be detected with the 1B11 monoclonal antibody. **(D-G)** 4C $CD4^+$ T cells were labeled with proliferation dye and transplanted into lethally irradiated MHC-mismatched CBF1 ($H\text{-}2K^{b/d}$) recipients receiving titrated doses of anti-Dll1/4 Abs. Glycoform-specific flow cytometric analysis of CD43 was performed on day 6 on fully divided 4C T cells. Dll1/4 blockade (αDll1/4) induced dose-dependent downregulation of the percentage of $1B11^{hi}$ 4C T cells **(D-E)** and 1B11 staining intensity (**F**, left panel), without loss in overall CD43 abundance (S11 staining intensity) (**F**, middle panel). The core-2 glycosylation status of CD43 could be examined on a single-cell basis by calculating a ratio of 1B11/S11 staining intensity (**F-G**). **(H-K)** Purified $CD4^+$ 4C or 4C-dnMAML were transplanted into CBF1 recipients as in (D). Proliferated alloreactive T cell subsets were assayed for 1B11 **(H)**, S11, 1B11/S11 ratios (**I)** and CD25 **(J)**. Among 4C-dnMAML T cells 1B11 reactivity was blunted in both $CD25^+$ and $CD25^-$ populations **(K)**. **(L)** Wild-type 4C T cells mixed 1:1 with 4C-dnMAML T cells were co-cultured on OP9-DL1 or OP9-DL4 stromal cells and stimulated in vitro with LPS matured bone-marrow-derived dendritic cells from poly(I:C)-induced Mx-Cre^+ $Dll1^{f/f}Dll4^{f/f}$ mice. Either OP9-DL1 or DL4 could increase core-2 CD43 O-glycosylation in a Notch ligand-dependent fashion. Mean and one standard deviation plotted in bar graphs. **p<0.01, ***p<0.001 by Student's *t*-test (B, H, J), one-way (E, G) or two-way (L) ANOVA with post-hoc Tukey's tests to assess differences in means.

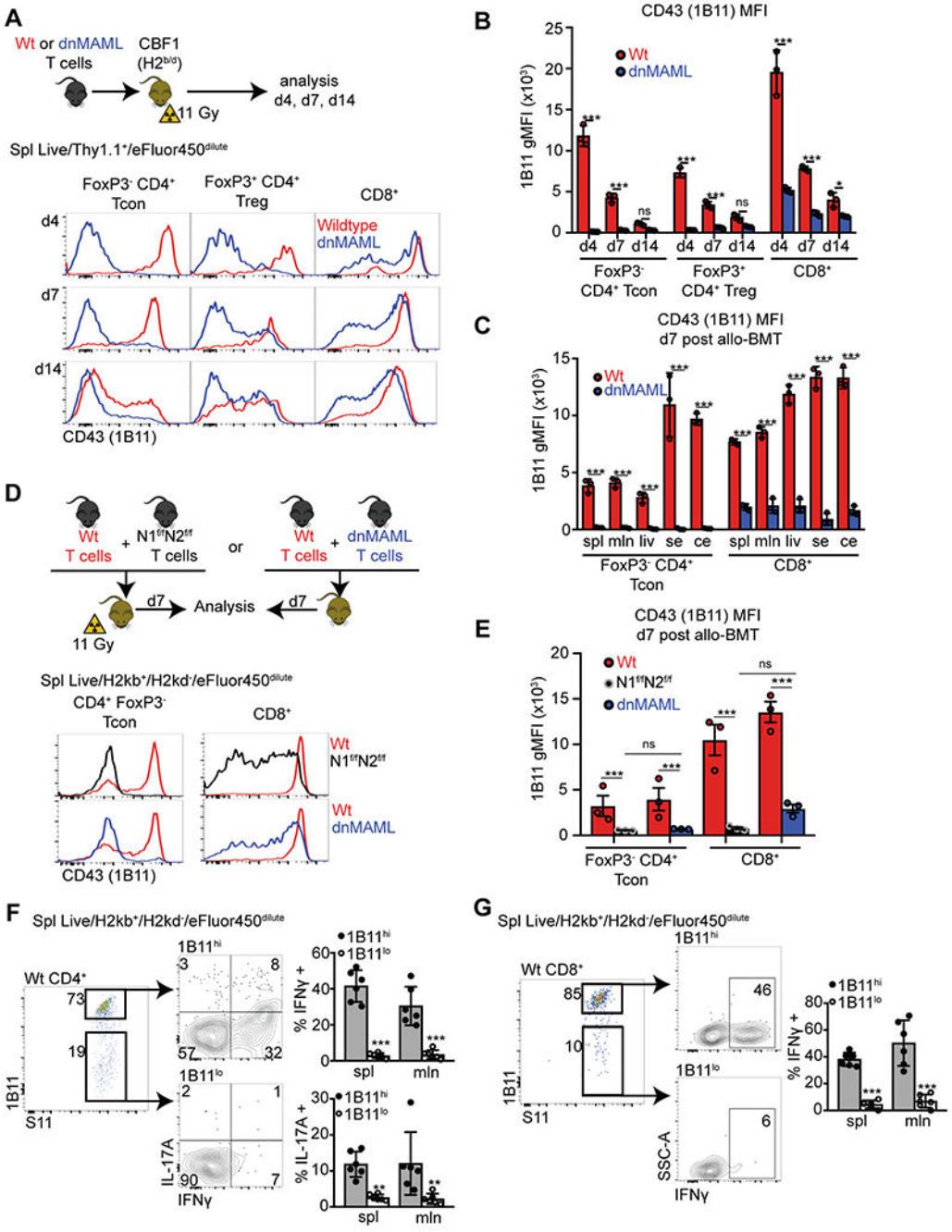

Figure 2. CD43 core-2 O-glycosylation requires cell-intrinsic canonical Notch signals in multiple alloreactive polyclonal T cell subsets.

(A-C) 5×10^6 purified B6 (H-$2^{b/b}$, Thy$1^{1/2}$) wild-type or dnMAML T cells were labeled with eFluor450 proliferation dye and transplanted separately into lethally irradiated (11 Gy) MHC-mismatched CBF1 (H-$2^{b/d}$, Thy$1^{2/2}$) recipients with analysis at day 4, 7 and 14. Core-2 O-glycosylation of CD43 in proliferated FoxP3^{-}CD4^{+} Tconv, FoxP3^{+} Treg, and CD8^{+} T cells was blunted by dnMAML-mediated Notch blockade at day 4 and day 7 **(A-B)**, both in secondary lymphoid organs and GVHD target tissues **(C)**. **(D-G)** 2.5×10^6 B6 wild-

type plus 2.5 × 10^6 CD4-Cre$^+$ dnMAML-GFP T cells or 2.5 × 10^6 B6 wild-type plus 2.5 × 10^6 CD4-Cre$^+$ *Notch1* $^{f/f}$*Notch2* $^{f/f}$ *Rosa*^{eYPF} T cells were co-transplanted as in **(A)**. For both Notch1 $^{f/f}$ Notch2 $^{f/f}$ T cells and dnMAML T cells, 1B11 reactivity was significantly blunted in alloreactive CD4$^+$ T conv and CD8$^+$ T cells **(D-E)**. Among wild-type CD4$^+$ **(F)** and CD8$^+$ **(G)** cells, 1B11^{hi} status predicted inflammatory cytokine production. spl = spleen, mln = mesenteric lymph node, liv = liver, se = small intestinal epithelium, ce = colonic epithelium. **p<0.01, ***p<0.001, one-way ANOVA with Tukey's post-hoc-tests.

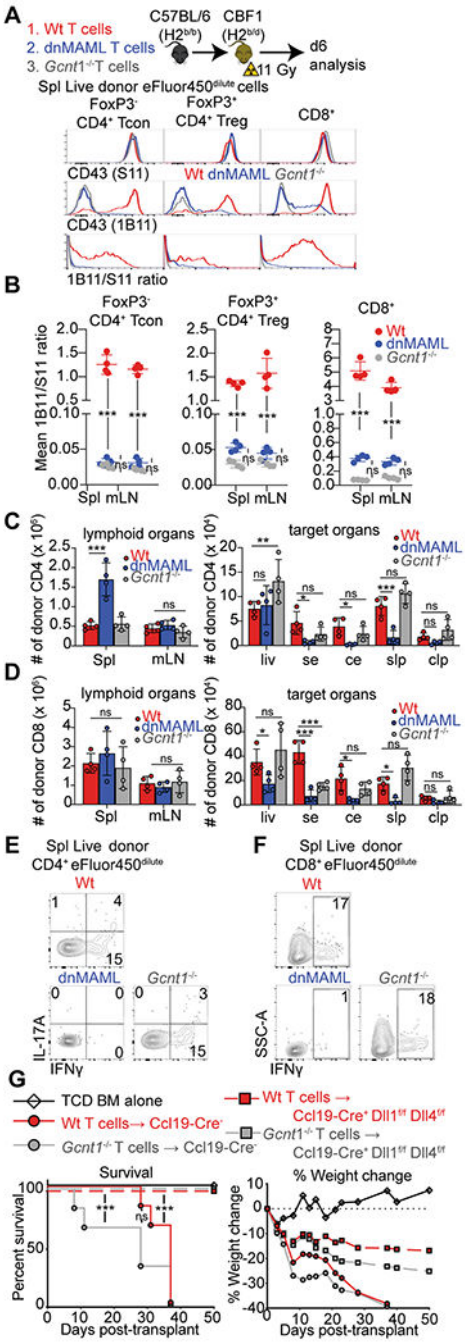

Figure 3. Notch blockade and *Gcnt1* loss abrogate CD43 core-2 O-glycosylation in alloreactive T cells, but *Gcnt1* loss does not decrease GVHD severity.

(A-F) 2.5×10^6 Wild-type, dnMAML, or *Gcnt1*$^{-/-}$ T cells (H-2$^{b/b}$) were transplanted into lethally irradiated CBF1 recipients (H-2$^{b/d}$) as in Fig 2. **(A-B)** Core-2 O-glycosylation of CD43 was monitored in lymphoid organs by flow cytometry at day 6. dnMAML CD4$^+$ Tconv fully recapitulated, while dnMAML CD4$^+$ Treg and CD8$^+$ T cells nearly fully recapitulated the loss of 1B11 reactivity seen in *Gcnt1*$^{-/-}$ T cells. Accumulation of alloreactive donor CD4$^+$ **(C)** and CD8$^+$ **(D)** T cells in lymphoid and GVHD target organs.

slp = small intestinal lamina propria. clp = colonic lamina propria. Cytokine production of representative alloreactive $CD4^+$ **(E)** and $CD8^+$ **(F)** T cell subsets. n=4 per group, flow panels from representative samples. **(G)** Survival and % weight change of lethally irradiated Ccl19-Cre^+*Dll1*$^{f/f}$*Dll4*$^{f/f}$ or Cre^- littermate control CBF1 recipients transplanted with 5×10^6 T cell-depleted bone marrow (TCD BM) plus 5×10^6 wild-type or *Gcnt1*-deficient T cells. n=6 per group from one experiment. *p<0.05, **p<0.01, ***p<0.001, one-way (B) or two-way (C, D) ANOVA with Tukey's post-hoc-tests. For (**G**), a log-rank test was used to compare groups.

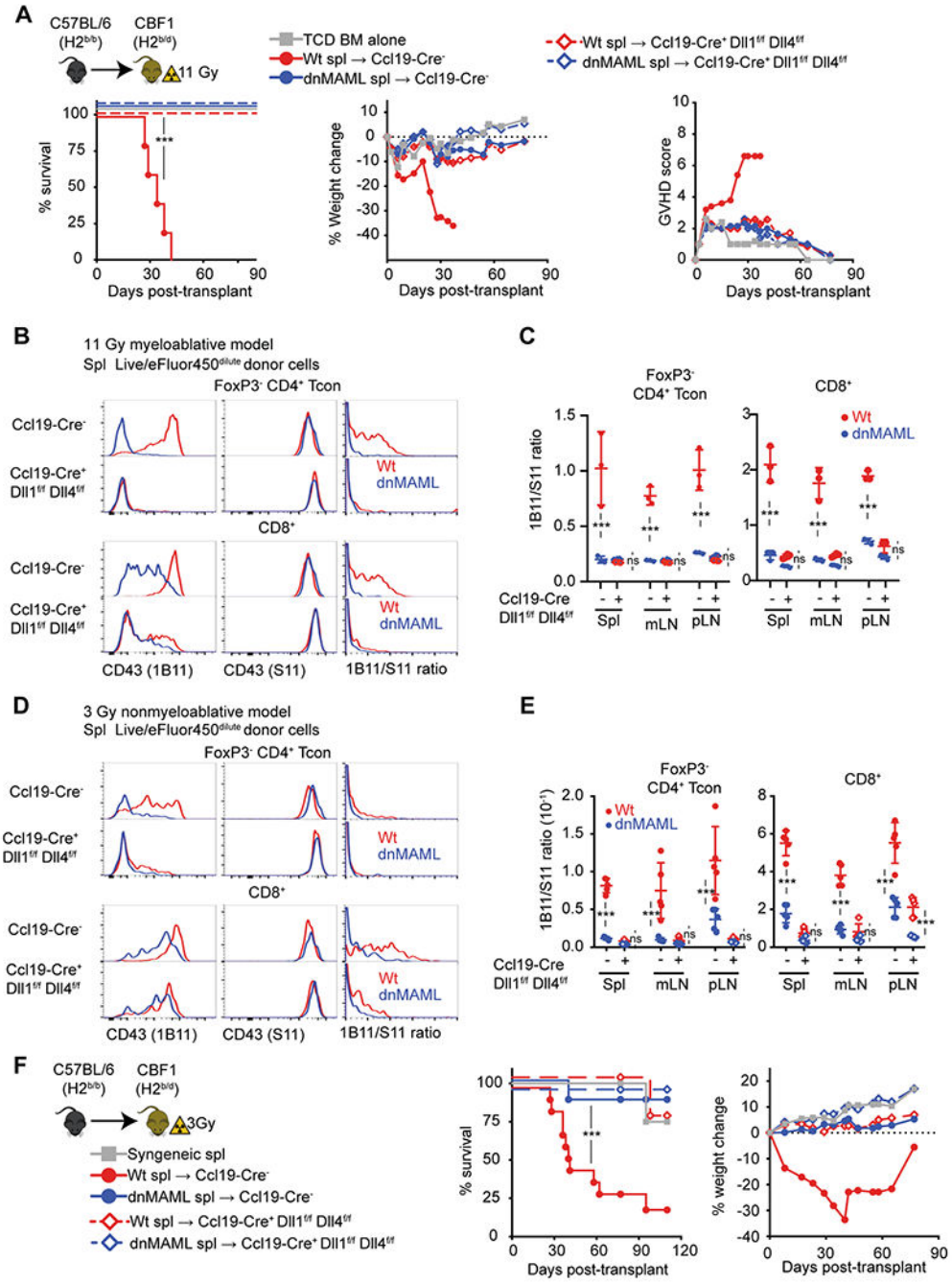

Figure 4. CD43 core-2 O-glycosylation reports Notch-dependent alloreactivity and identifies the critical Ccl19-Cre^{+} fibroblastic cell source of Delta-like ligands in GVHD.

(A) Survival, % weight change, and clinical GVHD score of lethally irradiated (11 Gy) Ccl19-Cre^{+} *Dll1$^{f/f}$Dll4$^{f/f}$* vs. Cre^{-} littermate control CBF1 recipients transplanted with 5 × 10^{6} TCD BM and 2 × 10^{7} wild-type or dnMAML splenocytes. n=5 mice per group, data representative of two independent experiments. **(B-C)** Flow cytometric analysis of CD43 core-2 O-glycosylation in co-transplanted wild-type and dnMAML T cell subsets harvested from Ccl19-Cre^{+} *Dll1$^{f/f}$Dll4$^{f/f}$* or Cre^{-} littermate controls at day 6 post-transplant. **(D-E)**

Flow cytometric analysis of CD43 core-2 O-glycosylation as in **(B-C)**. **(F)** Survival and % weight change in a non-myeloablative model of allo-BMT (3 Gy) where recipients received 4×10^7 splenocytes. Survival curve represents pooled data from three independent experiments of n=5 mice per group. Weight loss data are shown from one experiment. *p<0.05, **p<0.01, ***p<0.001, (A,F) log-rank test and (C,E) two-way ANOVA with Tukey's post-hoc-tests.

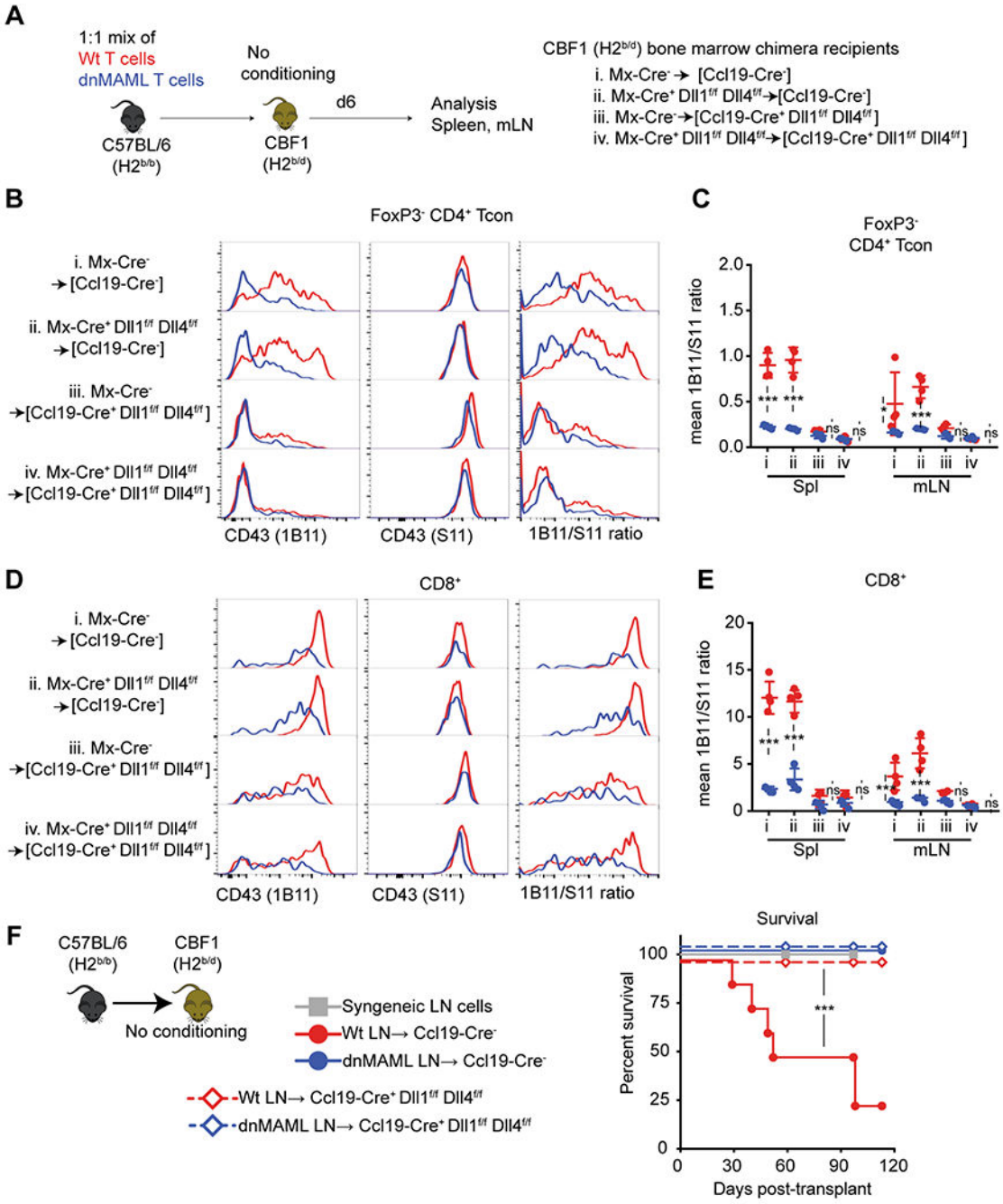

Figure 5. CD43 core-2 O-glycosylation in alloreactive T cells identifies a critical role for Ccl19-Cre$^+$ fibroblastic cells as a source of Delta-like ligands even in the absence of prior conditioning.

(A) Experimental scheme. Four-way bone marrow chimeras were generated by transplanting bone marrow from poly(I:C) induced Mx-Cre$^+$ *Dll1$^{f/f}$Dll4$^{f/f}$* or *Cre*- CBF1 littermate controls into syngeneic Ccl19-Cre$^+$*Dll1$^{f/f}$Dll4$^{f/f}$* or Cre$^-$ littermate controls. After 8 weeks of reconstitution, recipients received a donor lymphocyte infusion of 5×10^6 purified wild-type and 5×10^6 dnMAML T cells. Flow cytometric analysis of core-2 O-glycosylation of CD43 in alloreactive CD4$^+$ Tconv **(B-C)** and CD8$^+$ T cells **(D-E)**. **(F)** Survival of non-irradiated

Ccl19-Cre^{+}*Dll1*$^{f/f}$*Dll4*$^{f/f}$ or Cre^{-} littermate control CBF1 recipients transplanted with 60 × 10^6 wild-type or dnMAML B6 lymph node cells. Survival data are from two pooled independent experiments with a total of n=8 mice per group. *p<0.05, **p<0.01, ***p<0.001, (C,E) two-way ANOVA with Tukey's post-hoc-tests and (F) log-rank tests.

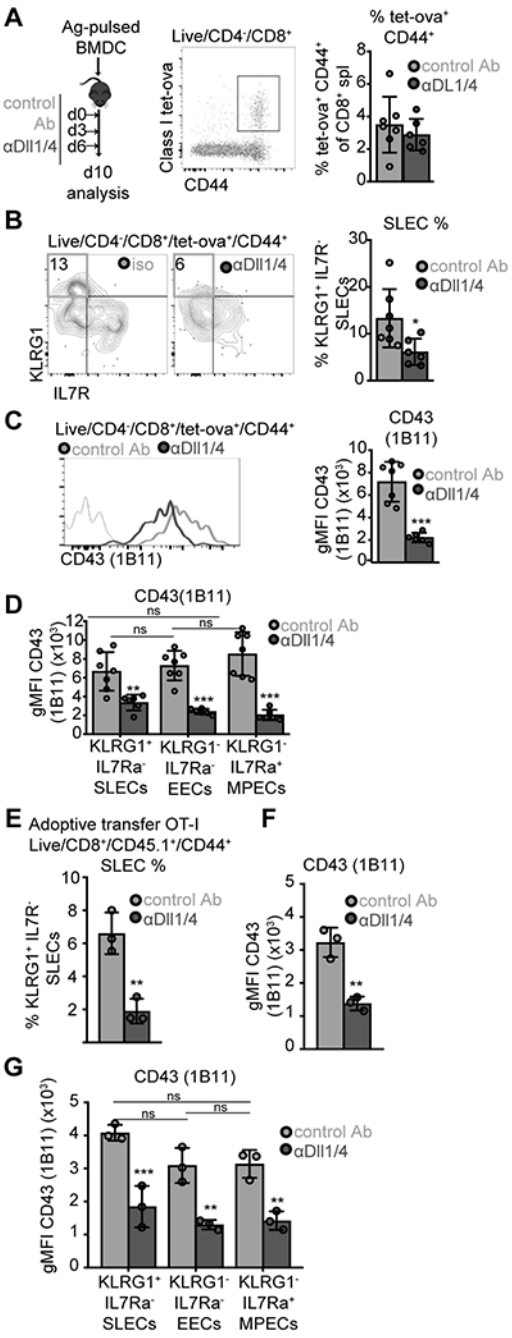

Figure 6. Delta-like Notch ligands drive KLRG1$^+$ short-lived effector T cell differentiation and CD43 core-2 O-glycosylation in antigen-specific CD8$^+$ T cell subsets after dendritic cell immunization.

(A-D) B6 mice treated with anti-Dll1/4 or isotype control antibodies were immunized with 5 × 10^5 bone marrow-derived dendritic cells (BMDC) pulsed with OVA peptide (SIINFEKL). Antigen-specific CD8$^+$ T cells were monitored by flow cytometry with K^b-OVA tetramer. **(A)** Blockade of Delta-like ligands did not negatively affect the expansion of antigen-specific CD8$^+$ T cells, but markedly blunted differentiation into KLRG1$^+$IL7R$^-$ short-lived effector cells (SLECs). **(B)** Abundance of the CD43 core-2 O-glycoform in bulk antigen-

specific $CD8^+$ T cells **(C)** or in SLEC, $KLRG1^-ILR7^-$ early effector cell (EEC), and $KLRG1^-ILR7^+$ memory precursor cell (MPEC) subsets **(D)**. Data representative of two experiments with n=6 mice per group. **(E-G)** BMDC immunization was performed as in **(A-D)**, but mice received 5×10^4 purified $CD45.1^+$ OT-I $CD8^+$ T cells by adoptive transfer one day before immunization. Data are representative of two experiments with n=3 mice per group. *p<0.05, **p<0.01, ***p<0.001, (A-C, E-F) student's *t*-test and (D-G) two-way ANOVA with Tukey's post-hoc-tests.

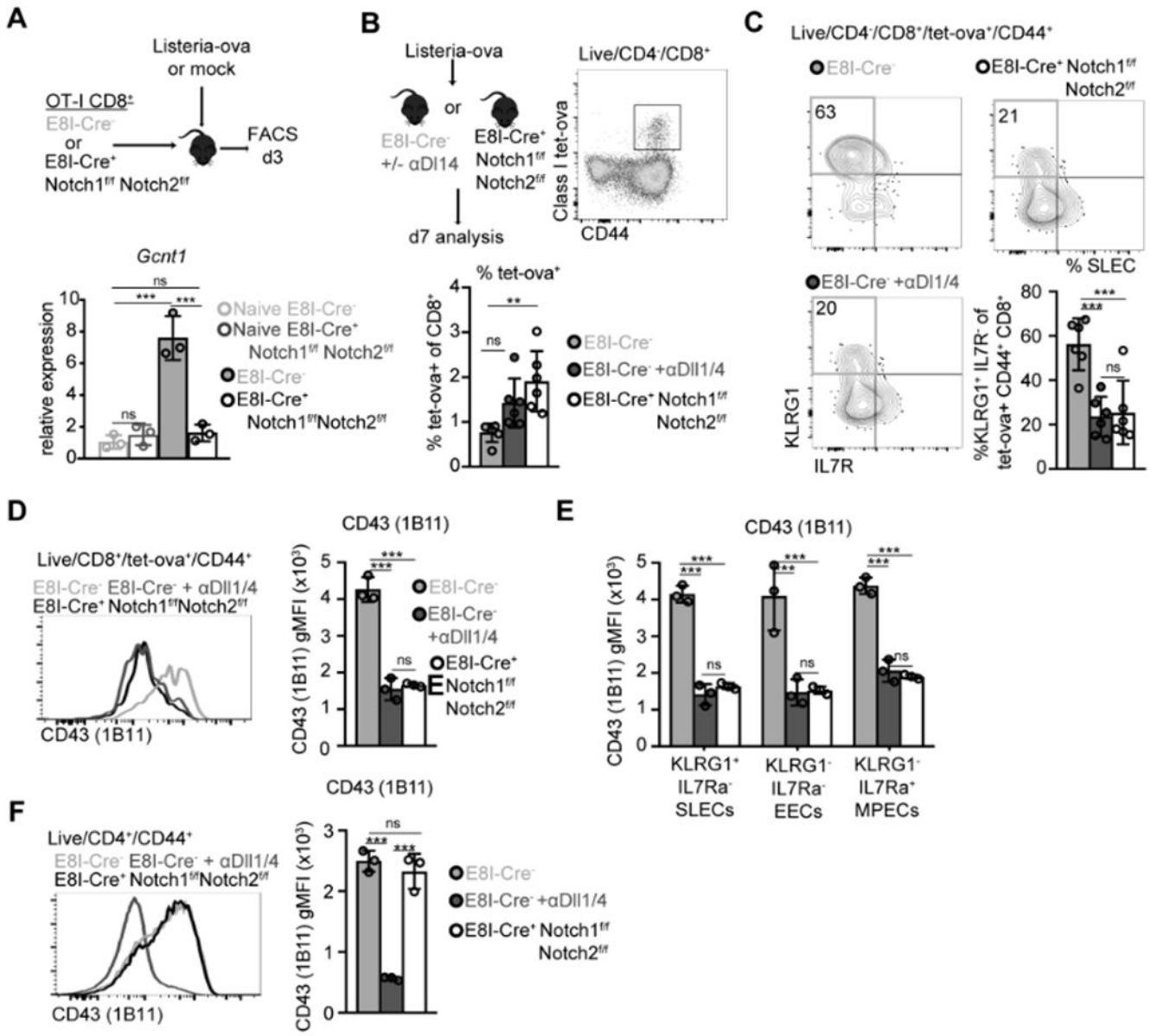

Figure 7. Delta-like Notch ligands control CD43 core-2 O-glycosylation in antigen-specific CD8$^+$ T cells during immune response to *Listeria* infection.

(A) 10^6 purified wild-type or E8I-Cre$^+$ *Notch$^{f/f}$ Notch2$^{f/f}$* CD8$^+$ OT-I (CD45.2$^+$) cells were transplanted into B6-CD45.1 recipients followed by infection with *Listeria monocytogenes* expressing ovalbumin (Lm-OVA) or mock infection. On day 3 post-infection, activated CD8$^+$CD45.2$^+$CD44^{hi} T cells were sorted from infected mice and naïve CD8$^+$CD45.2$^+$CD44^{lo} T cells were sorted from non-infected mice followed by analysis for *Gcnt1* mRNA by qRT-PCR. **(B-F)** Wild-type or E8I-Cre$^+$ *Notch$^{f/f}$ Notch2$^{f/f}$* mice were infected with a sublethal dose of 2×10^3 CFUs of Lm-OVA. A subset of wild-type mice received anti-Dll1/4 antibodies. The antigen-specific CD8$^+$ T cell response was monitored as in Fig. 6 (Fig. 7B). SLEC differentiation **(C)** and core-2 O-glycosylation of CD43 **(D)** depended on intact Dll1/4-mediated Notch signals and expression of the Notch1/2 receptors

in $CD8^+$ T cells. Notch-dependent core-2 O-glycosylation of CD43 was independent of early differentiation state in $CD8^+$ T cells **(E)** and also affected $CD4^+$ T cells, as activated $CD44^+CD4^+$ T cells showed decreased 1B11 reactivity in mice treated with anti-Dll1/4 antibodies, but not mice lacking Notch receptors only in $CD8^+$ T cells **(F)**. Data representative from two-independent experiments of n=3 per group. *p<0.05, **p<0.01, ***p<0.001, one-way (A-D, F) or two-way (E) ANOVA with Tukey's post-hoc-tests.